T-3266

THE DECAY OF SWIRLING-TURBULENT FLOW

by

Susan Ellen Feely McManus

A thesis submitted to the faculty and the Board of Trustees of the Colorado School of Mines in partial fulfillment of the requirments for the degree of Master of Science (Chemical Engineering and Petroleum-Refining).

Golden, Colorado

Date 11/26/86

Signed: SE McManus

Susan E. Feely McManus

Approved: M C Jones.

Dr. Michael C. Jones

Thesis Advisor

A J Kidnay

Golden, Colorado

Date 11/21/86

Dr. Arthur J. Kidnay

Department Head

Chemical Engineering

and Petroleum Refining

ABSTRACT

New measurements of the decay of turbulent, swirling flow are described. This work was sponsored by the Gas Research Institute. Swirl angles and velocity profiles were measured at four axial locations along seventy diameters of 100 mm (4 inch) smooth pipe. The swirling fluid was nitrogen gas at 4.1 MPa (600 psi) and ambient temperature.

Several theoretical and experimental investigations of the decay of swirl documented in the literature are reviewed. The different methods of measuring and describing the decay of swirl are described. The use of long lengths of pipe to attenuate swirl and restore a classical velocity profile is experimentally evaluated. A finite difference model of the decay phenomenon is shown.

TABLE OF CONTENTS

TABLE OF NOMENCLATURE

C - velocity coefficient (dimensionless)

d - orifice plate bore diameter (m)

D - diameter of pipe (m)

f - friction factor (dimensionless)

Δp - differential pressure (kPa)

K - angular momentum flux (N•m)

M - axial momentum flux (N)

P - pitch or twist rate (revolutions/diameter) (1/m)

P - pressure (MPa)

r - radial distance from the center of rotation (m)

R - radius of pipe (m)

Re - pipe Reynolds number = ρUm D/μ (dimensionless)

Sn - swirl number (dimensionless)

U - axial component of velocity (m/s)

Um - average axial velocity (m/s)

Vp - velocity vector (m/s)

W - tangential velocity vector (m/s)

x - axial distance (m)

Y - radial distance from center of pipe (m)

β - decay parameter (dimensionless)

ε - eddy diffusivity (m^2/s)

μ - fluid viscosity (Pa•s)

ν - kinematic viscosity (m^2/s)

ρ - fluid density (kg/m^3)

θ - swirl angle (degrees)

ω - average angular velocity (1/sec)

* - dimensionless quantity

LIST OF FIGURES

LIST OF TABLES

ACKNOWLEDGEMENTS

The author would like to express her sincere appreciation to Mr. Doug Mann and Mr. Jim Brennan for initiating this thesis program and for their guidance, encouragement and support throughout this work.

The technical guidance and advise of Dr. Michael Jones is greatly appreciated.

Charlie Sindt, Isaura Vazquez-Pantoja, Blaine Bateman, Nick Sanchez, and Gary McFaddin contributions of technical advise and graphical expertise during this work is also appreciated.

The financial support provided by the Gas Research Institute is gratefully acknowledged.

Special gratitude is expressed to my parents for all the opportunities and encouragement throughout my life.

I INTRODUCTION

Swirling flow is a vortex motion about a center of rotation. In a classical definition of fully developed, turbulent, compressible pipe flow, the velocity vector is exclusively in the axial direction. In swirl, tangential and radial components of velocity are induced. For symmetric swirls the rotation occurs about the pipe axis. The complexity of the classical turbulent compressible flow model is further increased by the introduction of swirl. Because of the non-linearities in the Navier-Stokes equations describing fluid motion and the insufficient understanding of the nature of turbulence, many assumptions and empirical parameters have to be used to reach numerical models. In order to understand the phenomenon of swirl, this research program was undertaken to experimentally characterize a turbulent, nonsymmetric swirl and determine the decay rate as a function of pipe length. The experimental results are compared to the results of a numerical model previously developed by Fejer [1]. The experimental initial conditions were used in the numerical model.

Swirl can be generated in engineering systems by compressors, valves and various piping configurations. Potential benefits of swirl include increasing mass transfer and heat tranfer rates. In flow measurement, swirl can have a significant adverse affect on a flowmeter's performance. Kinghorn [2] reviewed the research of many investigators and reported changes in discharge coefficient of several flowmeters including flow nozzles, orifice and venturi meters. As much as a 40 percent change in the discharge coefficient of an orifice meter was measured at large swirl angles. Bean [3] showed the effect of a number of piping configurations on the discharge coefficient of an orifice meter.

Orifice meters are commonly used in flow measurement because they are inexpensive and do not require individual calibration. For a given geometry and fluid, in undisturbed flow conditions, the mass flow rate can be determined from measurements of the fluid temperature, static pressure and the differential pressure across the orifice plate.

Measurements of orifice meter discharge coefficients made at the National Bureau of Standards show significant changes in the orifice coefficient in swirling flow [4]. Figure 1 shows the performance of a 4 inch orifice flowmeter with a 2 inch plate. The mass flow rate deviation is the deviation from the mass flow rate determined from several calibrations of the meter against a standard. Based on this study, 33 degrees of swirl were

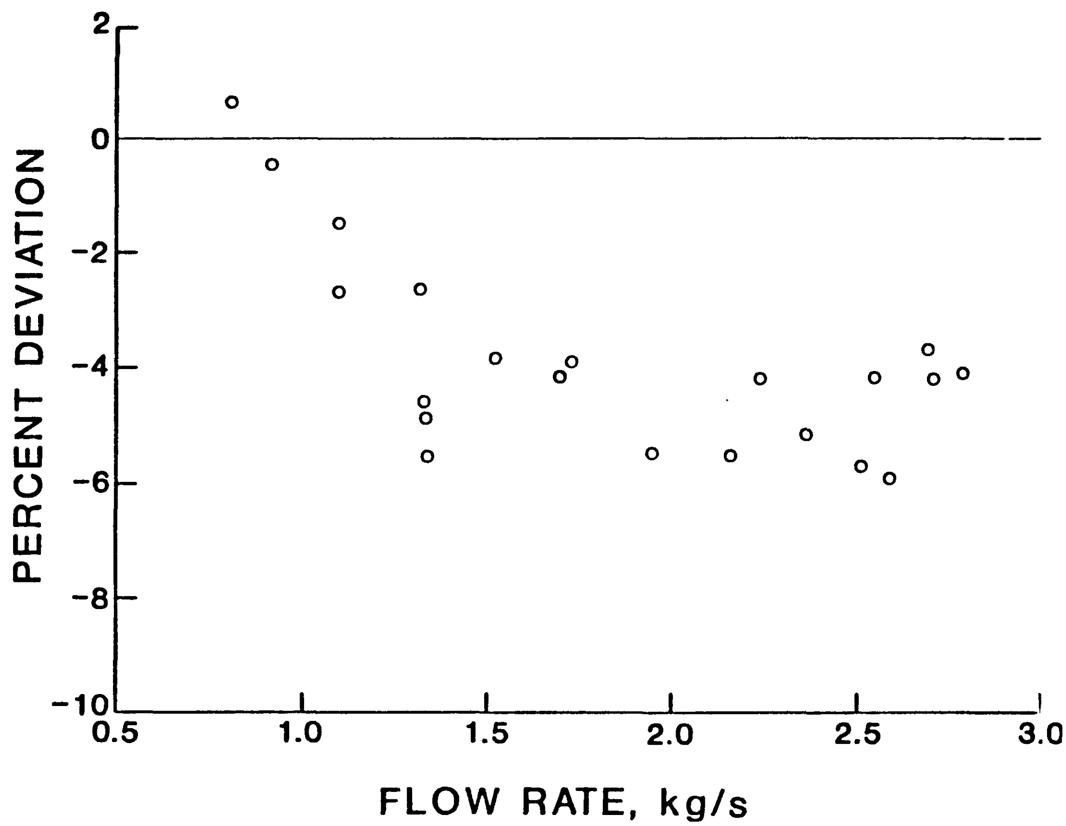

Figure 1. Performance of a 100 mm (4 inch) orifice meter in swirling flow

calculated to be present at the meter. Fifty-four diameters of straight pipe preceeded the meter for the data shown here. The current gas industry standard [5] specifies that 25 diameters (@ d/D= 0.50) of straight pipe is necessary upstream of an orifice meter to sufficiently remove flow disturbances so that the flow measurement uncertainty will be within the tolerance of the standards. For the case shown here, the standard [5] was insufficient to remove the swirl and the meter under registered an average of about 4.5 percent at flow rates above a pipe Reynolds number of 1,000,000. The error was also significantly flow rate dependent.

The most common way of removing swirl and restoring a classical fully developed turbulent velocity profile is by installing sufficient pipe length upstream of the flowmeter so that the distortions in the flow are dissipated by viscous and turbulent forces. In this study, the decay of swirl was measured in a 100 mm (4 inch) pipe at four axial locations extending 70 pipe diameters. The flow characteristics of interest were the swirl angles, velocity profiles, and angular momentum flux profiles.

A discussion of swirling flow follows, along with a review of previous researcher on the decay of swirl. The experimental section contains a discussion of the apparatus used to measure swirl and experimental results are reported. The results of an explicit numerical model are reported. Comparisions are made between several researchers.

II LITERATURE REVIEW

Musolf [6] experimented with the decay of turbulent swirling flow of water in 25 mm (1 inch) and 51 mm (2 inch) smooth pipes. He assumed the axial velocity profile did not change from the non-swirling to the swirling flow conditions. The swirl was measured with a straight vaned rotor and the swirl angle was obtained with a directional pitot tube. The static pressure was measured at the wall and an equation was developed for the pressure drop caused by decaying swirl. A decay equation was given as a function of pipe Reynolds number and axial distance. He concluded that the axial distance necessary for swirl to decay was twice as long for turbulent flow as for laminar flow.

Krieth and Sonju [7] developed an analytical decay equation as a function of an axial distance and Reynolds number. The Reynolds number was based on the radius of the pipe and the maximum radial value of the axial velocity instead of the pipe diameter and bulk velocity. This diffenece makes the comparison of their decay equations with other researchers difficult. The axial velocity was assumed constant in the axial direction and was a 1/7 power law profile in the radial direction.

Krieth and Sonju [7] found their correlation was in good agreement with Musolf's [6] water data for the Reynolds number range of 20,000 to 120,000. They concluded that the decay was faster at lower Reynolds numbers. The eddy diffusivity was assumed a constant in the radial and axial position.

Fejer, Lavan and Wolf [1] extensively researched the decay of swirl in air in a 76 mm (3 inch) smooth pipe. Their investigation of the eddy diffusivity gradients and density gradients revealed a strong dependence on both radial and axial position. The decay of angular momentum was empirically fit to an exponential decay equation as a function of Reynolds number and axial distance. The radius of maximum swirl and maximum tangential velocity decreased with axial distance. The dependence of the decay rate on the initial swirl intensity was shown to be almost negligile as compared to the Reynolds number dependence.

Nissan and Bresan [8] investigated swirling water flow in a smooth, vertical pipe. Swirl was induced by two tangential jets at the closed end of a pipe. With the use of a pitot tube and a static pressure probe, they found the radial component of velocity to be much smaller than the other velocity components. At a tangential velocity of 1.2 m/s (4 ft/s) and an axial velocity of 0.9 m/s (3 ft/s), the radial component was 0.03 m/s (0.1 ft/s). The radial static pressure profile became more uniform as the tangential velocity profile decayed.

Baker [9] and Baker and Sayre [10] studied the decay of swirl in water and viscous hydrocarbons with a straight vaned rotor and a pitot-static tube in 146 mm (5.75 inch) and 30 mm (1.18 inch) smooth pipes. Reynolds numbers ranged from 12,500 to 200,000. Baker [9] suggested the dependence of the decay rate on the inlet swirl intensity but was unable to verify this. The decay rate decreased as the Reynolds number increased. The largest pressure gradients were in the radial direction as compared with the axial direction.

Mottram and Rawat [11] developed an analytical decay equation as a function of the friction factor. Their model assumes a flat axial velocity profile and that the maximum swirl angle occurs close to the wall. Experimental measurements of the swirl angle and velocities were made in air in an 80 mm pipe with two different surface finishes. Significant changes in the decay rate were shown to be caused by surface finish. The effect of swirl on an orifice meter's discharge coefficient with different upstream pipe roughness is also shown.

III SWIRL CHARACTERIZATION

Figure 2 shows a three dimensional cross-section of a pipe. The vector notation illustrates the relationship of the velocity vector to the pipe axis. The individual components can be resolved by:

$$Vp = C(\rho\Delta p)^{1/2} \tag{1}$$

$$U = Vp\cos(\theta) \tag{2}$$

$$W = Vp\sin(\theta) \tag{3}$$

Swirling flow can be separated into two regimes as seen in figure 3. A forced vortex or solid body rotation results from inducing swirl with a fixed vaned rotor, pipe bend combinations or similar swirl generator. The swirl rotates with a constant angular velocity. The forced vortex decays because of viscous dissipation at the wall. The angular momentum and tangential velocity profiles decay as the fluid moves down the pipe. A radial static pressure gradient can results from the centrifugal force of the swirl.

The decay rate is usually quantified as the ratio of the swirl at a reference location to the swirl measured downstream. The reference location is usually the farthest upstream location where the swirl was measured. There are two common ways of

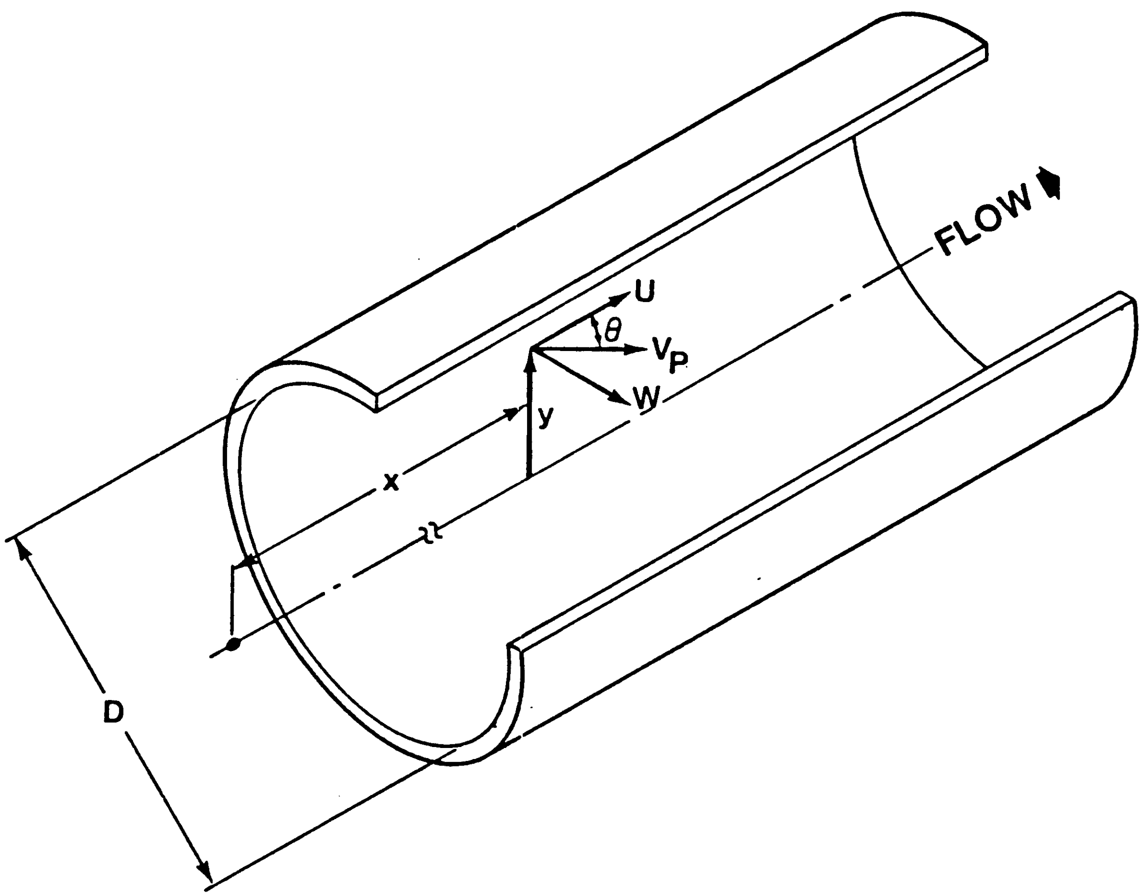

Figure 2. Vector coordinates for swirl analysis

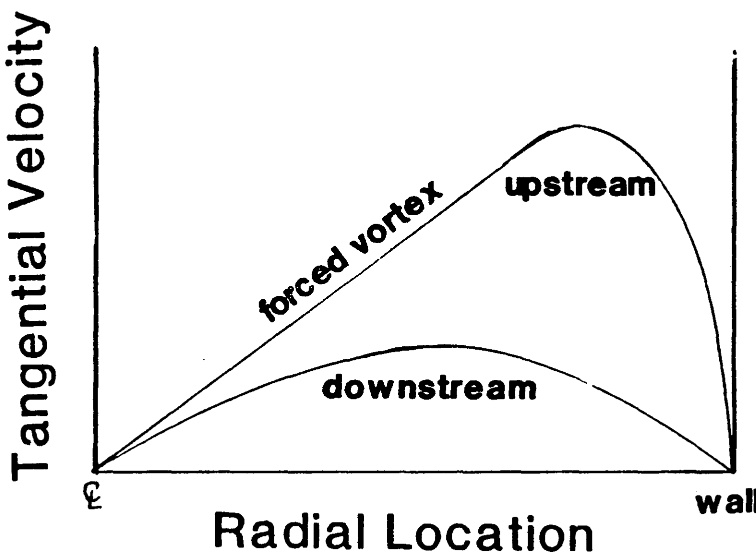

Figure 3. Characteristics of swirling flow properties (Based on Baker [9])

quantifing this rate of decay. When the angular momentum flux is measured, the decay rate is expressed as the ratio of the angular momentum flux at a downstream location to the angular momentum flux at the reference location.

$$\frac{K}{K_o} = \frac{2\pi\rho\int_0^{D/2} UWr^2\,dr \Big|_{x/D}}{2\pi\rho\int_0^{D/2} UWr^2\,dr \Big|_{x/D=0}} \qquad (4)$$

For experimental swirl measurements with a straight vaned rotor, where ω is defined as the average angular velocity of the rotor, the swirl decay is described by a quantity defined as the swirl number:

$$Sn = \omega/(U_m P/D) \qquad (5)$$

The decay is approximated by an exponential rate for both expressions and is of the form:

$$\frac{K}{K_o} = Sn = e^{-\beta x/D} \qquad (6)$$

In this form, β , has been found to be a strong function of Reynolds number below Reynolds numbers of 1,000,000 [1,6,9].

Mottram and Rawat's [11] analytical decay equation was derived for swirl that resembles a forced vortex, such that the maximum tangential velocity and swirl angle are close to the wall. This equation is:

$$\frac{K}{K_o} = \frac{(W_o/\bar{U})_{x/D}}{(W_o/\bar{U})_{x/D=0}} = \frac{2\ b\ e^{-4fx/D}}{b^2 - (W_o/\bar{U})^2_{x/D=0}\ e^{-8fx/D}} \qquad (7)$$

where

$$b = (1 + (W_o/\bar{U})^2)^{1/2}_{x/D=0} + 1 \qquad (8)$$

and W_o is the maximum tangential velocity. This expression can be related to the maximum swirl angle at each location by:

$$\tan(\theta_{max}) = W_o/\bar{U} \qquad (9)$$

Therefore equation (7) can be rewritten as:

$$\frac{K}{K_o} = \frac{\tan(\theta_{max})_{x/D}}{\tan(\theta_{max})_{x/D=0}} = \frac{2\ b'\ e^{-4fx/D}}{b'^2 - \tan^2(\theta_{max})_{x/D=0}\ e^{-8fx/D}} \qquad (10)$$

where

$$b' = (1 + \tan^2(\theta_{max}))^{1/2}_{x/D=0} + 1. \qquad (11)$$

This form of the decay equation relates the decay to the friction factor. Since the friction factor is a function of both the Reynolds number and pipe roughness, the equation includes the Reynolds number dependence seen in other research [1,6,9].

IV SWIRL MEASUREMENT INSTRUMENTATION

A common method of measuring swirl is with a straight vaned rotor or swirl meter. This device measures swirl rotation but does not resolve the individual velocity components. Flow visualization is another method of measuring swirl for low swirl angles. Velocity profiles can not be determined by flow visualization.

Hot wire and hot film anemometers are commonly used in dynamic flow measurements of velocity profiles and turbulence intensities. The anemometer must be calibrated often and is an intrusive instrument. For flows having a large amount of swirl, the direction of the velocity vector must be predetermined before making a measurement [12]. Since the anemometer output is proportional to the convective heat transfer, flow in all directions affects the output. On a cross wire anemometer the velocity vector must be greater than 30 degrees from each wire to obtain useful results within the calibration range.

Laser doppler anemometry (LDA) is a non-intrusive flow measurement instrument that can resolve velocity components and provide information on turbulence intensities. LDA provides direct measurement of velocities without calibration. If there is insufficient natural scattering source in the flow, seeding is necessary for scattering of the laser light.

Pitot tubes designed with two or more separate and isolated pressure ports are simple swirl angle indicators [13]. The pressure ports are located in a plane perpendicular to the pitot tube axis. On a two hole probe, when the two ports experience the same pressure, then the direction of the flow is assumed to be half way between the two ports. Like the hot wire anemometer, a pitot tube must be calibrated and is an intrusive instrument. Data in this study were taken using a three-hole pitot tube.

V EXPERIMENTAL PROCEDURE

The cryogenic flow measurement facility of the National Bureau of Standards in Boulder, Colorado was modified in 1979 to include a gas flow reference system [14]. In brief, the closed loop process begins with liquid nitrogen being pumped to 4.1 MPa (600psi). The high pressure fluid is then heated to ambient temperature in a series of two heat exchangers. As seen in figure 4, the flow exits the shell side of a baffled shell and tube steam heat exchanger in the vertical direction, descends 8.5 pipe diameters, goes through a right angle elbow into the horizontal plane of the gas flow test section. The heat exchanger and upstream piping configuration generate a large amount of swirl immediately following the flange on the elbow.

The test section, shown in figure 5, contains ports for a directional pitot tube and a temperature probe as well as static pressure taps. A manual traversing unit equipped with both linear and angle scales were attached to the pitot tube. The angle scale was preset so that at 0 degrees the impact pressure port on the pitot tube was directed upstream on the axis of the pipe. The test section spool piece was designed so that the pitot tube could be traversed across two axes of the pipe; 90 degrees from each other.

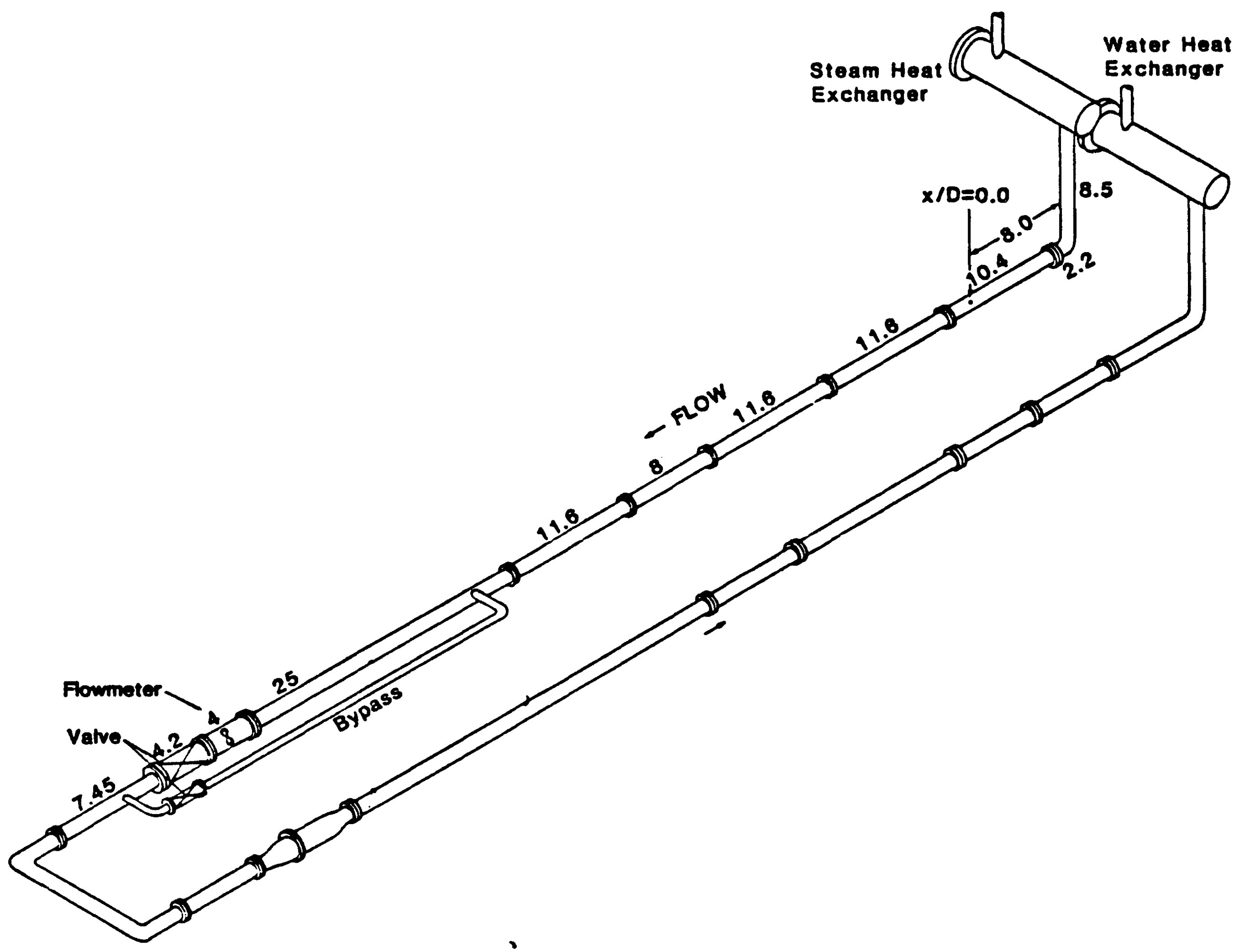

Figure 4. Piping configuration of gas flow test section

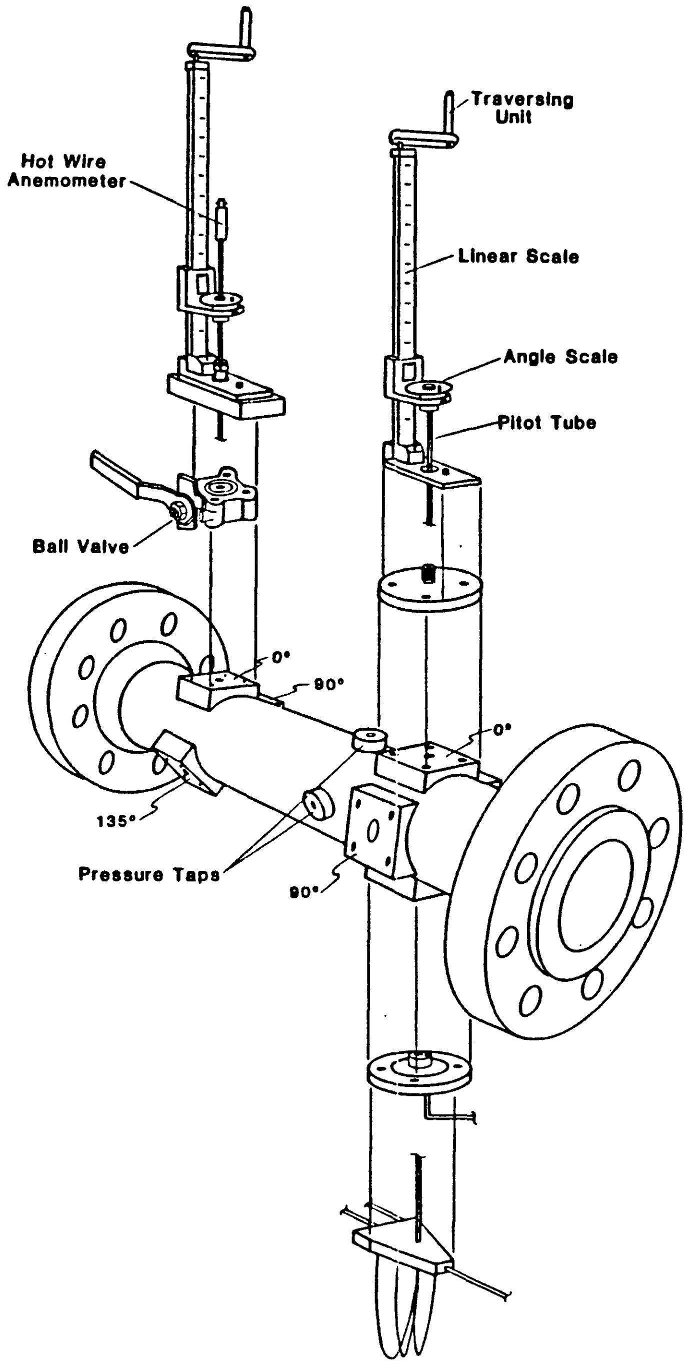

Figure 5. Instrumented spool piece for measuring swirl angles, velocities, pressures, and temperatures

The directional pitot tube (figure 6) has 3 separate and isolated pressure ports. The outside ports are 40 degrees from the center port. The center port was used to measure the impact pressure and the two outside ports are used to find the direction of the local velocity vector. The pitot tube was rotated about its axis until the differential pressure between the two outside ports was at a minimum. At this condition, the swirl angle was read from the angle scale on the traversing unit. A velocity was then determined from the differential pressure between the center pressure port and the wall static pressure. Because of the cylindrical design, the measured velocities had more scatter than a convential type design. The cylindrical design was used for accurate swirl angle measurements.

Three pressure transducers were used to measure 1)the differential pressure between the wall static pressure tap and the center tap on the pitot tube, 2) the differential pressure between the two outside ports on the pitot tube used to find the direction of flow and 3) the wall static pressure. A microcomputer and data acquisition hardware were used to digitize and record the output from the transducers. The computer was also used to record the time, temperature, radial position and angle of rotation. A minimum of 5 individual data points were recorded

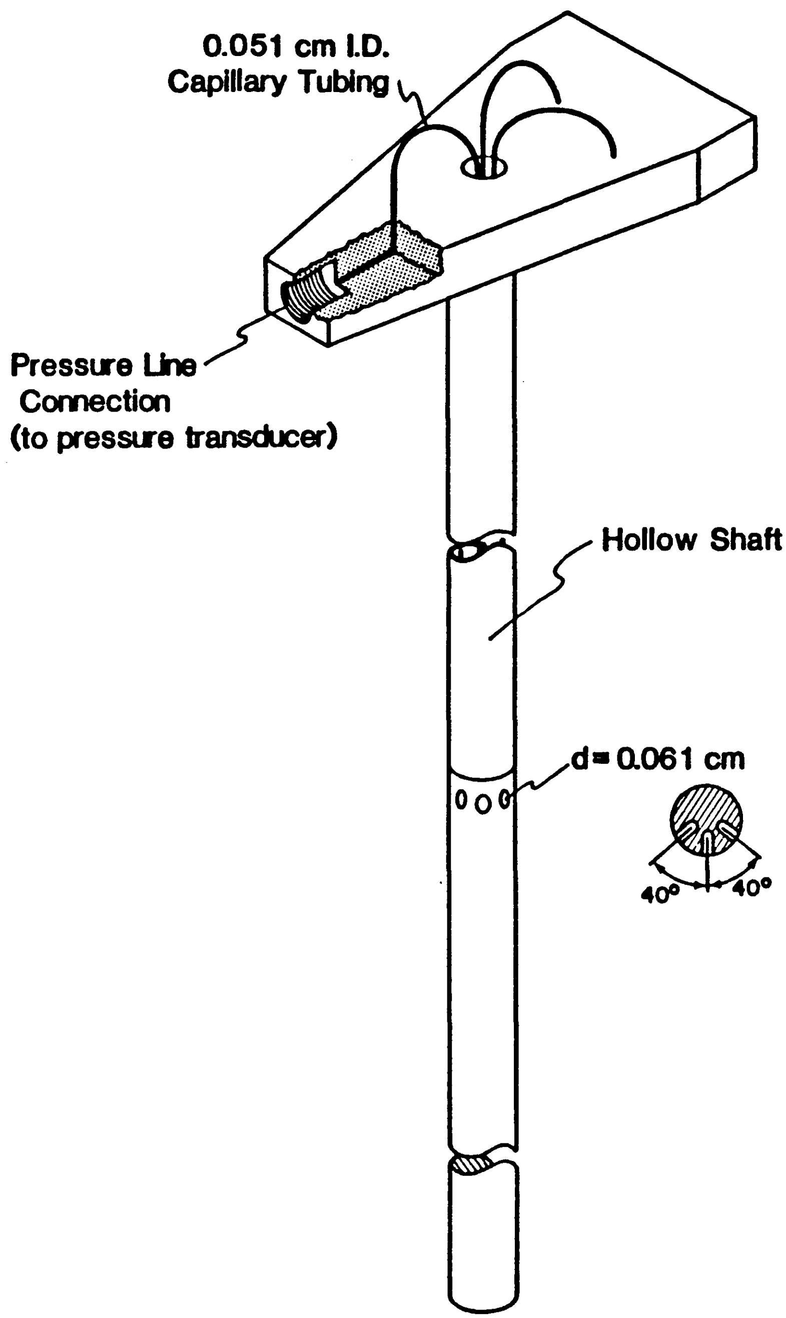

Figure 6. Directional pitot tube for the measurement of swirl anlgles and velocities

at each radial position. Usually the analog signals were averaged at a high sampling rate for 17-30 seconds.

The instrumented spool piece was inserted into the piping at four locations downstream of the right angle elbow (figure 4). The location with the spool piece inserted at the flange following the elbow is referred to as $x/D = 0.0$ where x is the distance from this reference location and D is the diameter of the pipe. The other locations were $x/D = 10.5$, 33.3, and 70.0.

VI EXPERIMENTAL RESULTS

Swirl angle profiles illustrate the magnitude and symmetry of the swirl in flow. Radial measurements of the swirl angles and velocity vectors were made at three flow rates which correspond to pipe Reynolds numbers of 800,000, 1,000,000 and 1,400,000.

Figure 7 shows the swirl angle profiles determined from the directional pitot tube at the x/D = 0.0 location. The abscissa (Y/R) is the radial location in the pipe with 1 and -1 representing the walls of the pipe. The swirl angle was measured from the axial velocity vector, U, (see figure 2). The sum of the absolute value of the maximum swirl angle on each side of the pipe is referred to as the magnitude of the swirl angle across the pipe. The magnitude of the swirl measured at x/D = 0.0 was 59 degrees across the pipe and the swirl was asymmetric. Measurements at the middle flow rate, Re = 1,000,000, were repeated several months later and the profiles agreed with each other to within the accuracy of the directional pitot tube of ± 2 degrees.

At the x/D = 10.5 location, profiles were measured as shown in figure 8. The magnitude of the swirl was approximately 49

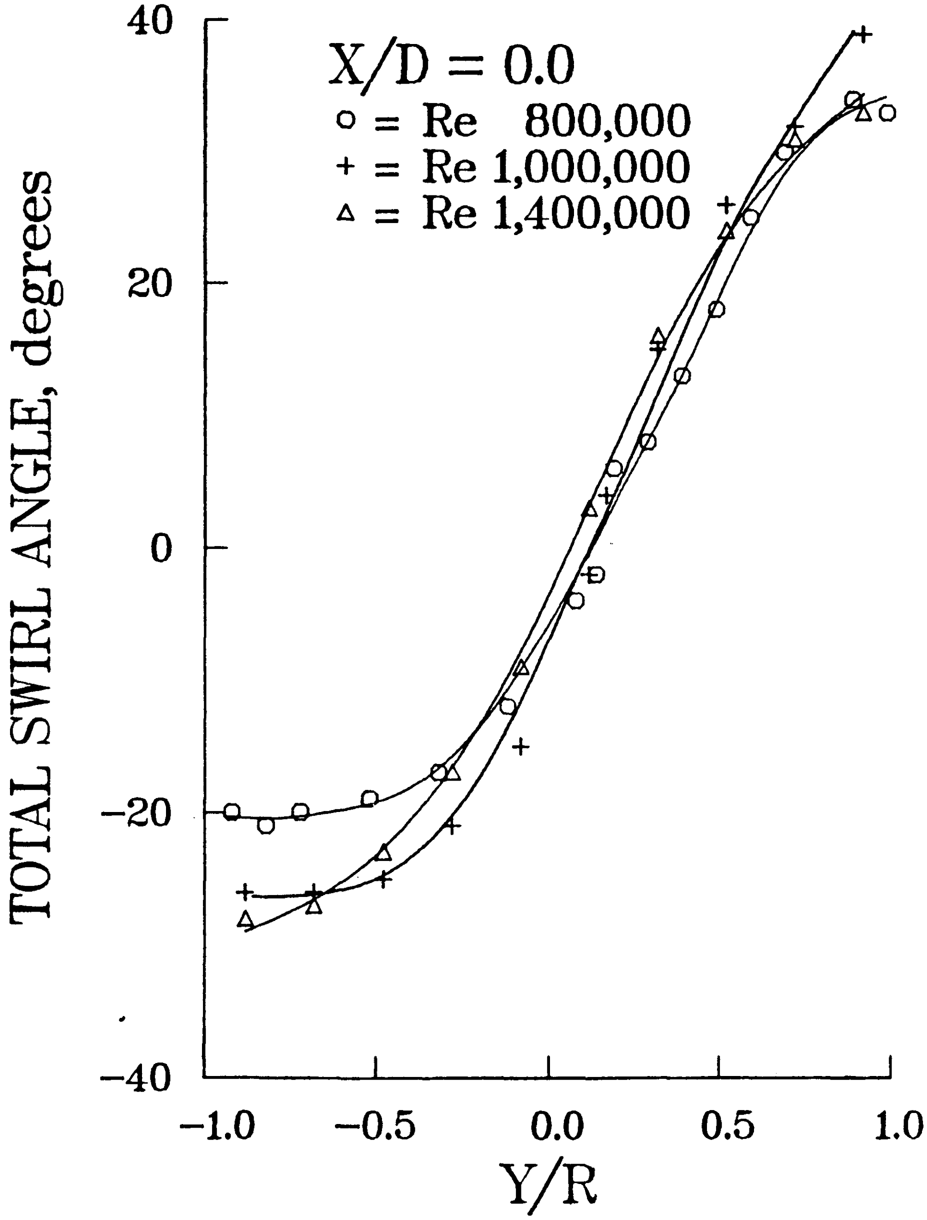

Figure 7. Swirl angle profile at x/D = 0.0

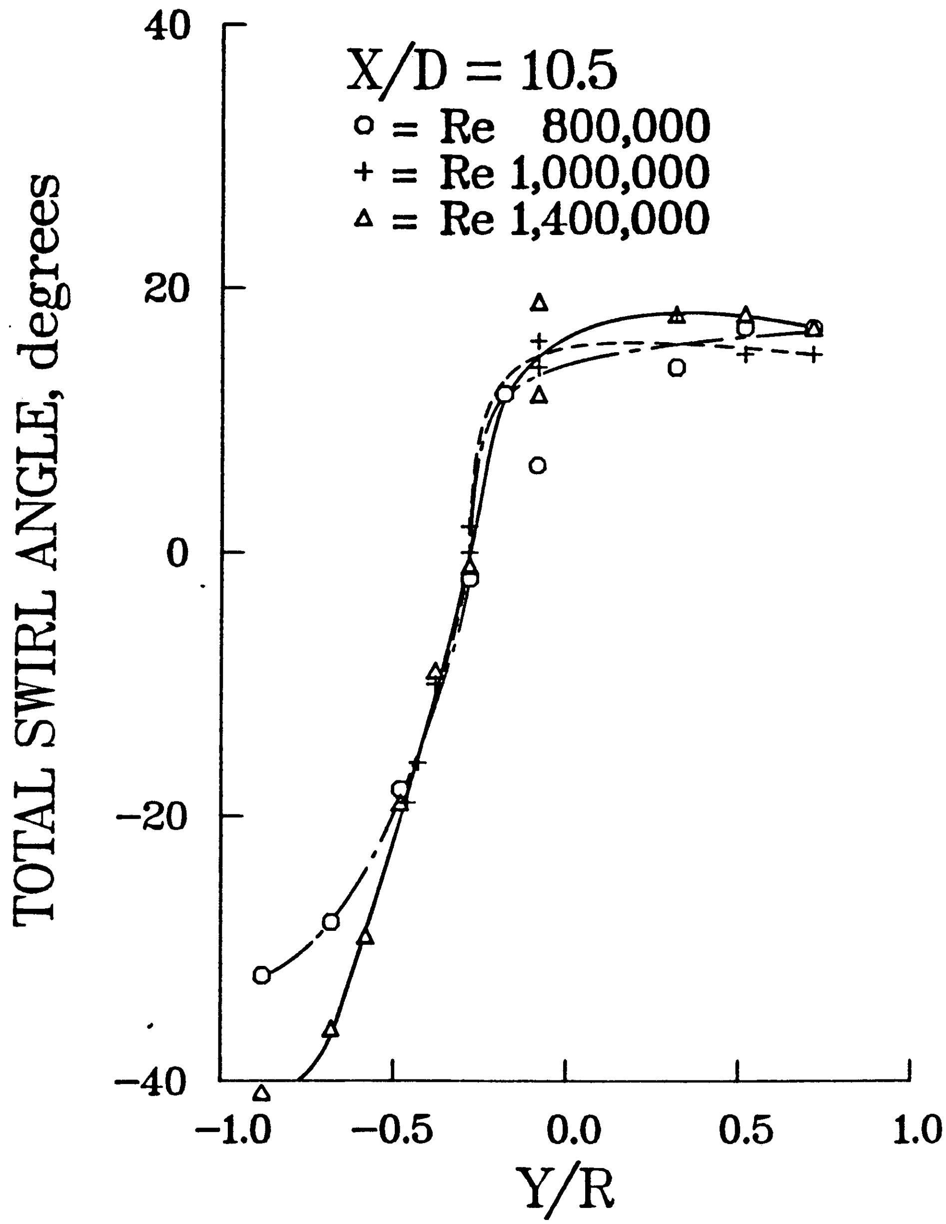

Figure 8. Swirl angle profile at x/D = 10.5

degrees across the pipe. This was a 22 percent decrease of the initial swirl (x/D = 0.0) and the swirl remained asymmetric. The apparent center of rotation changed between x/D = 0.0 to x/D = 10.5.

The swirl angle profile was nearly symmetrical at the x/D = 33.5 location. Traverses at x/D = 33.5 for all three Reynolds numbers are plotted in figure 9. At this location a pitot tube traverse was also made in the horizontal direction, in addition to the vertical direction where all the previous measurements were made, to confirm the symmetry of the swirl about the pipe axis. Figure 10 shows the swirl angle profiles in the horizontal plane where the characteristics are the same as in the vertical plane. The 34 degrees of swirl across the pipe represented a 43 percent decay from the x/D = 0.0 location.

At x/D = 70.0, the swirl was 24 degrees across the pipe which was a decay of 64 percent from x/D = 0.0. Figure 11 shows the swirl angles obtained at this location for Re of 1,000,000 and 1,400,000. Measurements were not made at this location for Re = 800,000.

Figure 12 shows the decay of the swirl at a Re = 1,000,000 from x/D = 0.0 to x/D = 70.0. Figure 13 shows the decay at a

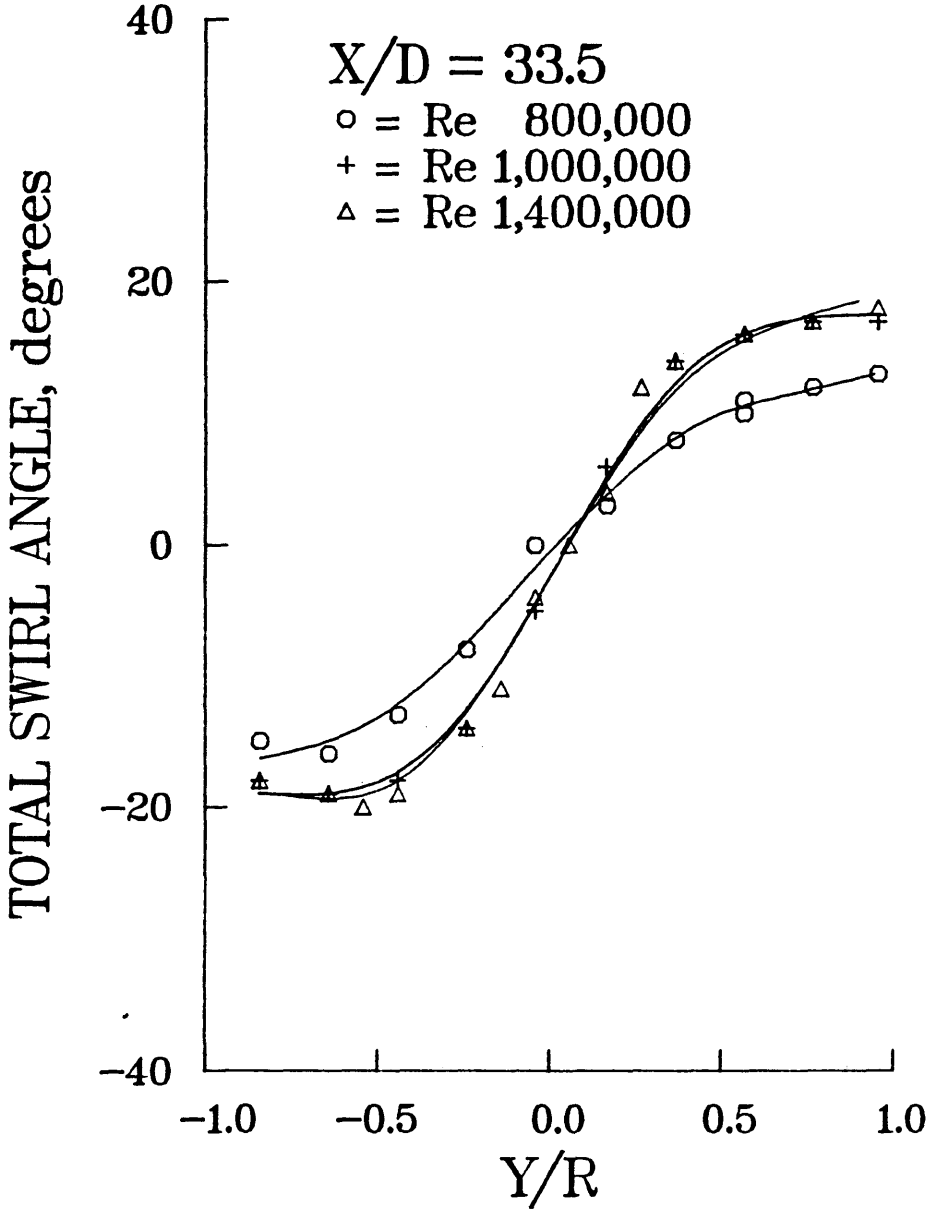

Figure 9. Vertical swirl angle profile at x/D = 33.5

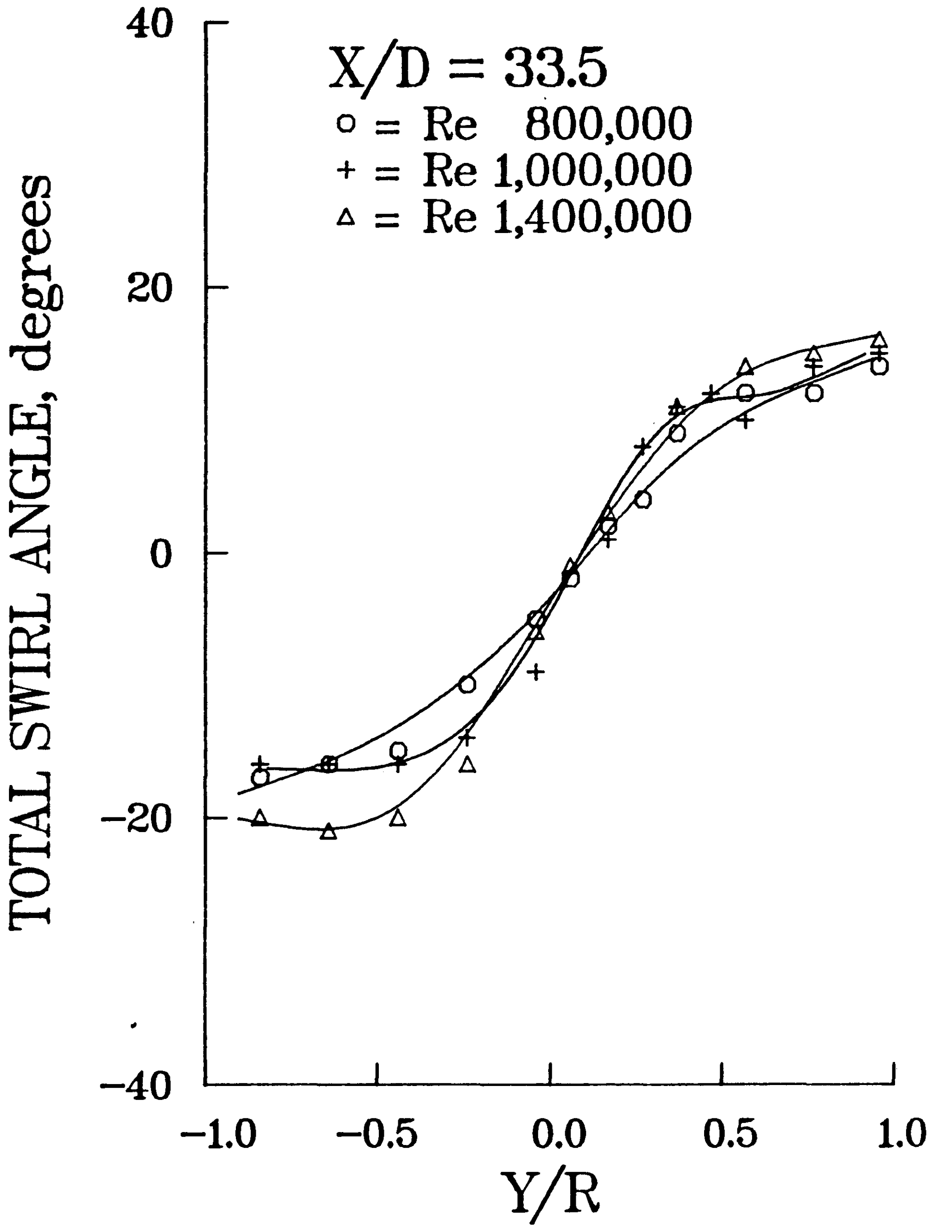

Figure 10. Horizontal swirl angle profile at x/D = 33.5

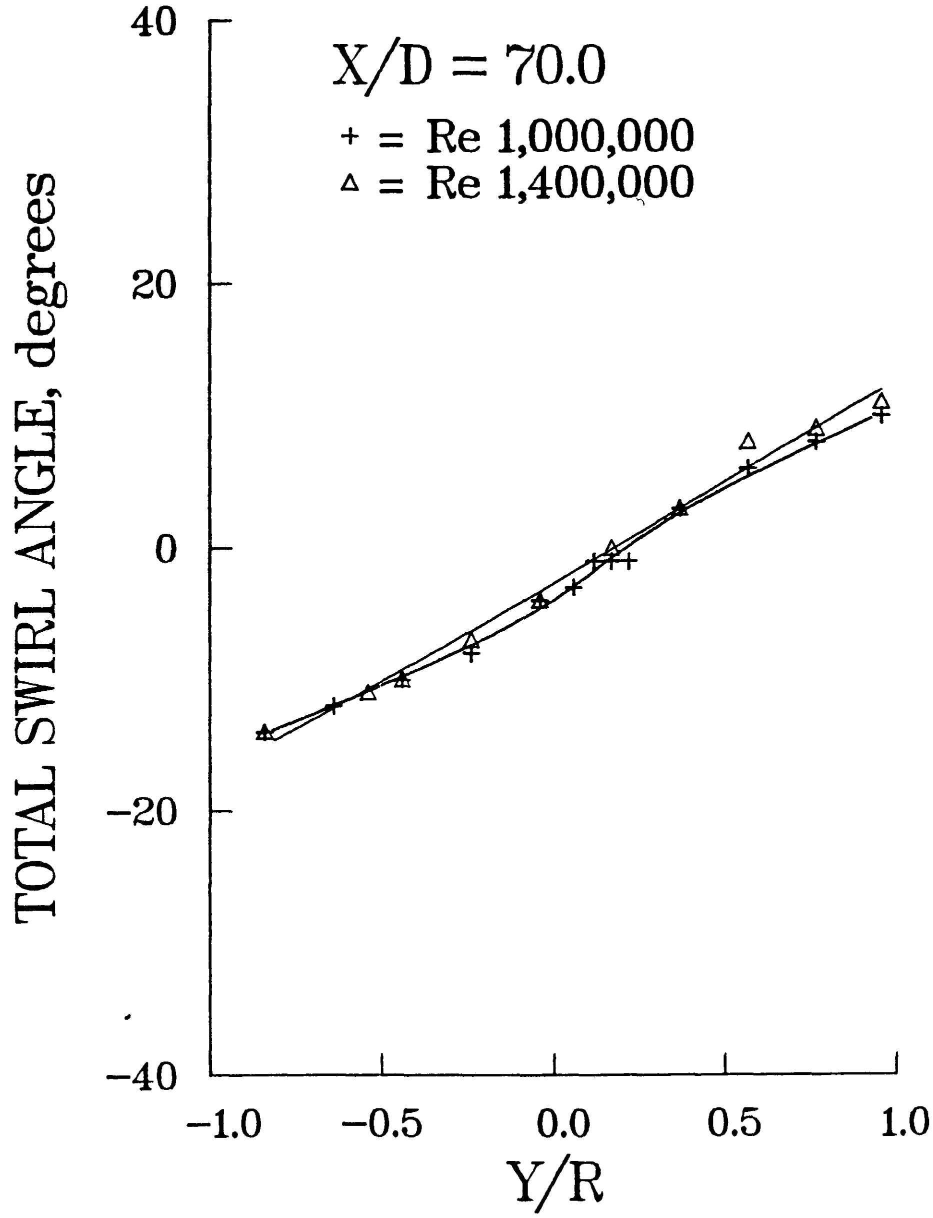

Figure 11. Swirl angle profile at x/D = 70.0

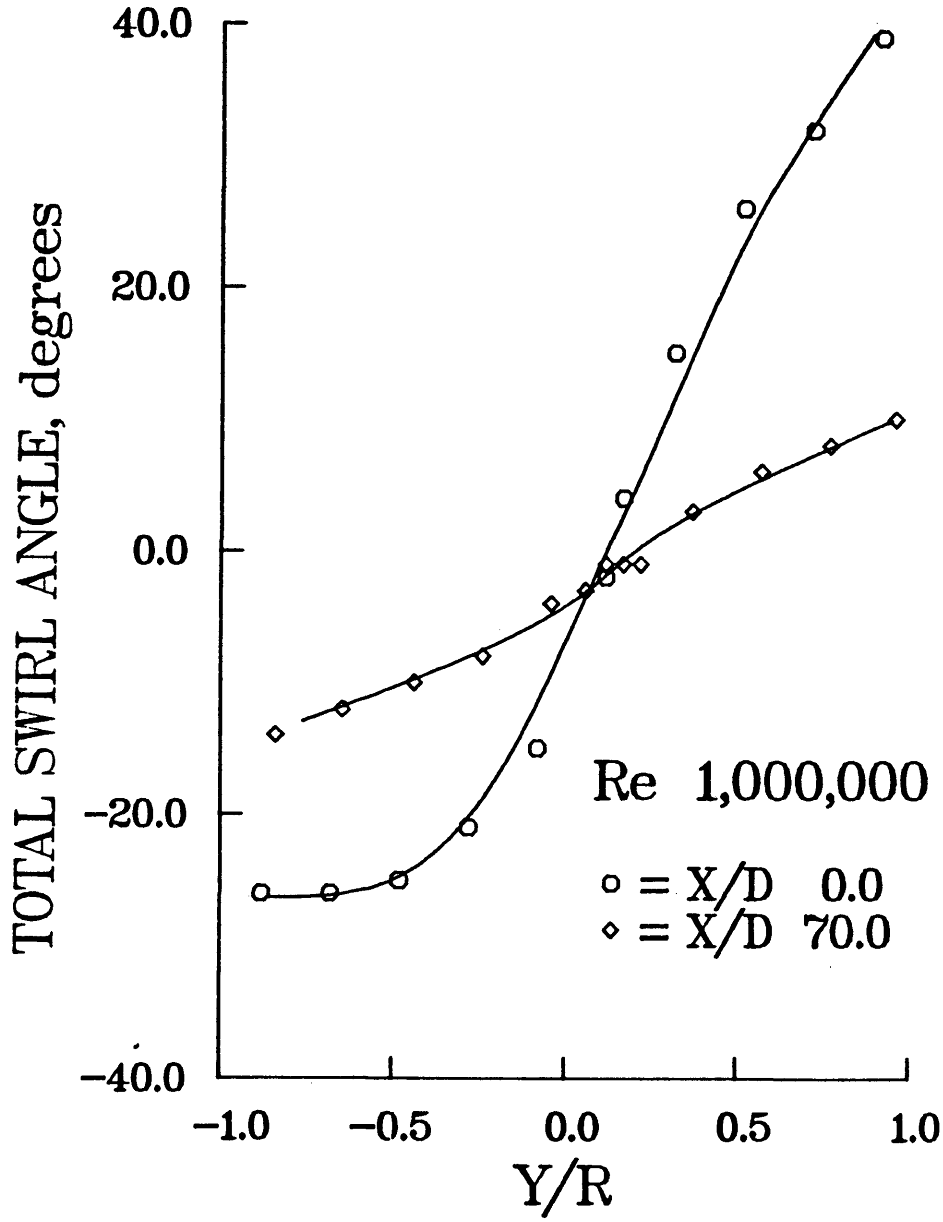

Figure 12. Swirl decay at Re = 1,000,000 from x/D = 0.0 to x/D = 70.0

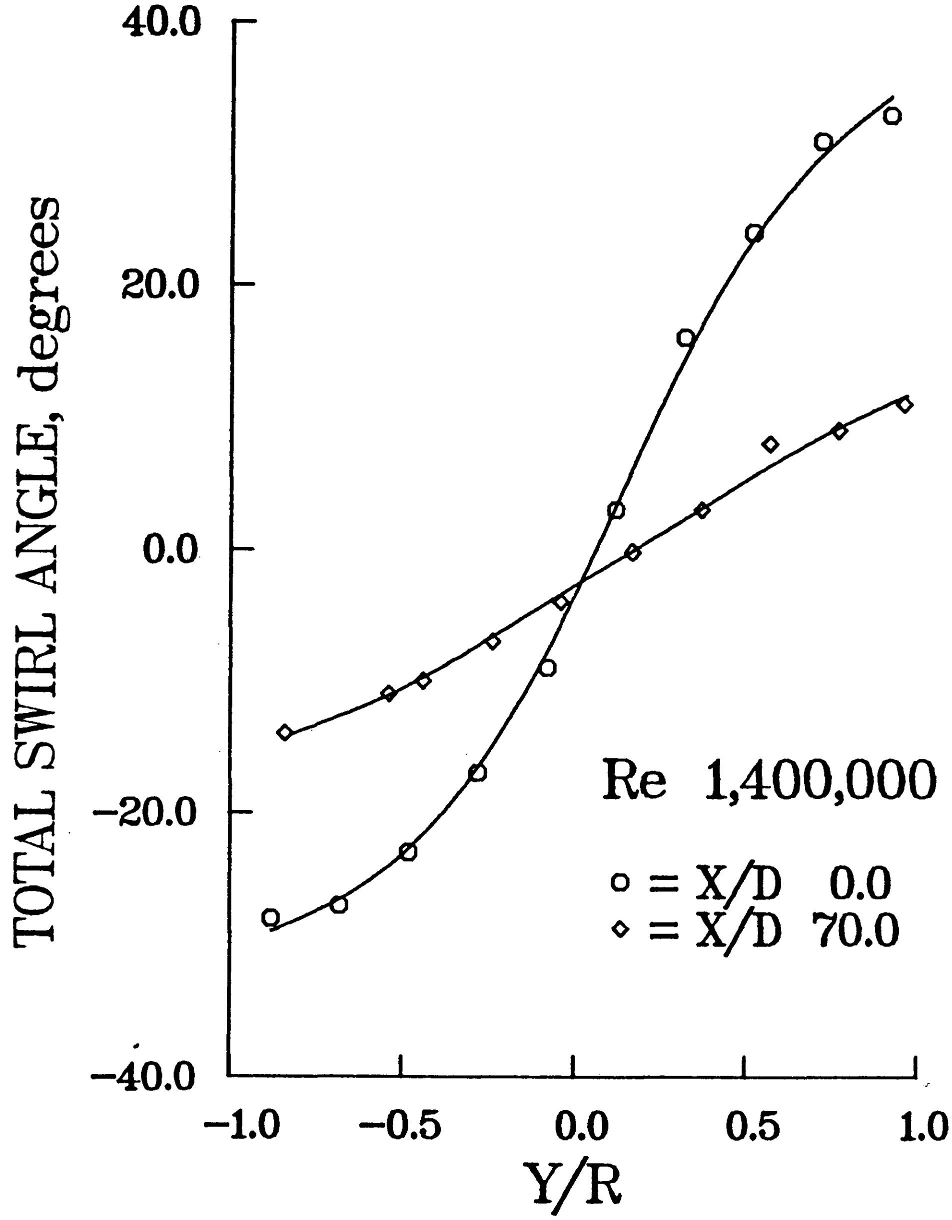

Figure 13. Swirl decay at Re = 1,400,000 from x/D = 0.0 to x/D = 70.0

Re = 1,400,000. Even though the swirl had decayed, a significant amount of swirl remained after seventy pipe diameters. The swirl resembles a forced vortex with the maximum swirl angle occuring close to the wall.

An important characteristic of swirling flow is the decay of angular momentum flux in the axial direction [1,6,9]. Figures 14 through 16 are plots of the angular momentum flux profiles at various Reynolds numbers. The average axial velocity, Um, was calculated from the mass flow rate as determined from the mass flow reference system. The axial and tangential velocities are normalized by the average axial velocity. The ordinates are a dimensionless form of the angular momentum flux. The center of rotation at x/D = 0.0 was calculated at Y/R = 0.17. At the 10.5D location the center of rotation was at the other side of the pipe at Y/R = -0.28. At the two other locations, x/D = 33.5 and 70, the swirl was nearly symmetric and therefore the center of rotation was taken at Y/R = 0.0.

The angular momentum flux profiles at Re = 800,000 are shown in figure 14. The swirl at x/D = 0.0 is asymmetric and the angular momentum is greater in the negative radial direction. At x/D = 10.5, the swirl is again asymmetric, but the angular momentum has shifted in the positive direction. The profile is

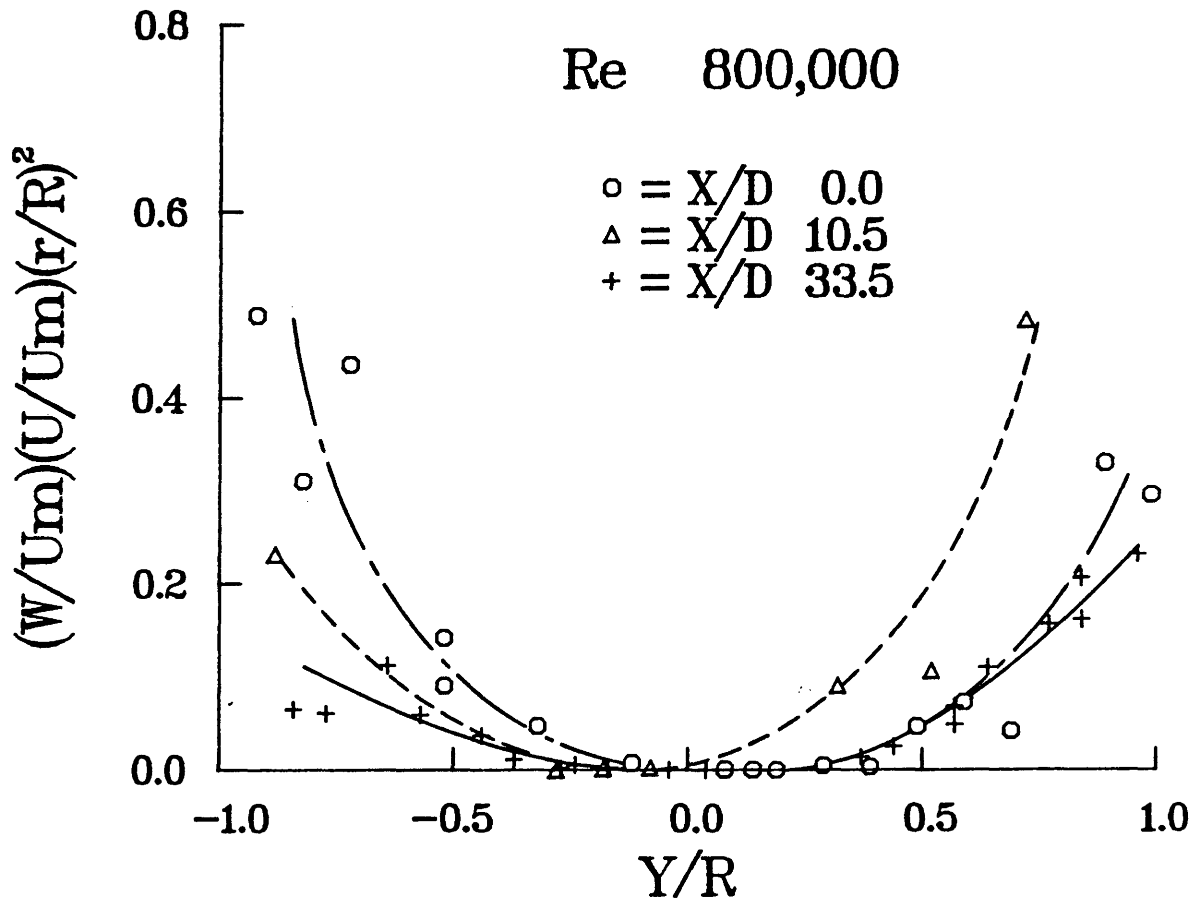

Figure 14. Angular momentum distribution at Re = 800,000

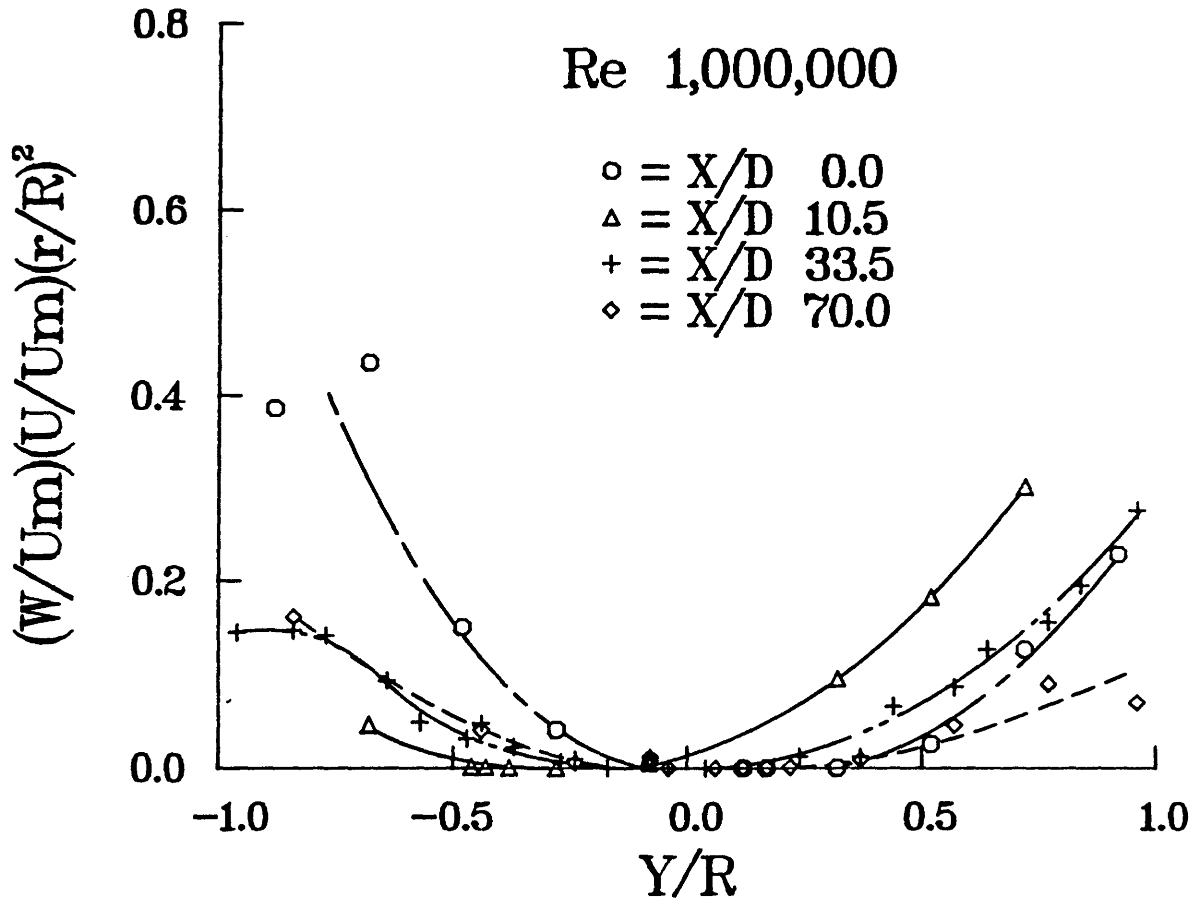

Figure 15. Angular momentum distribution at Re = 1,000,000

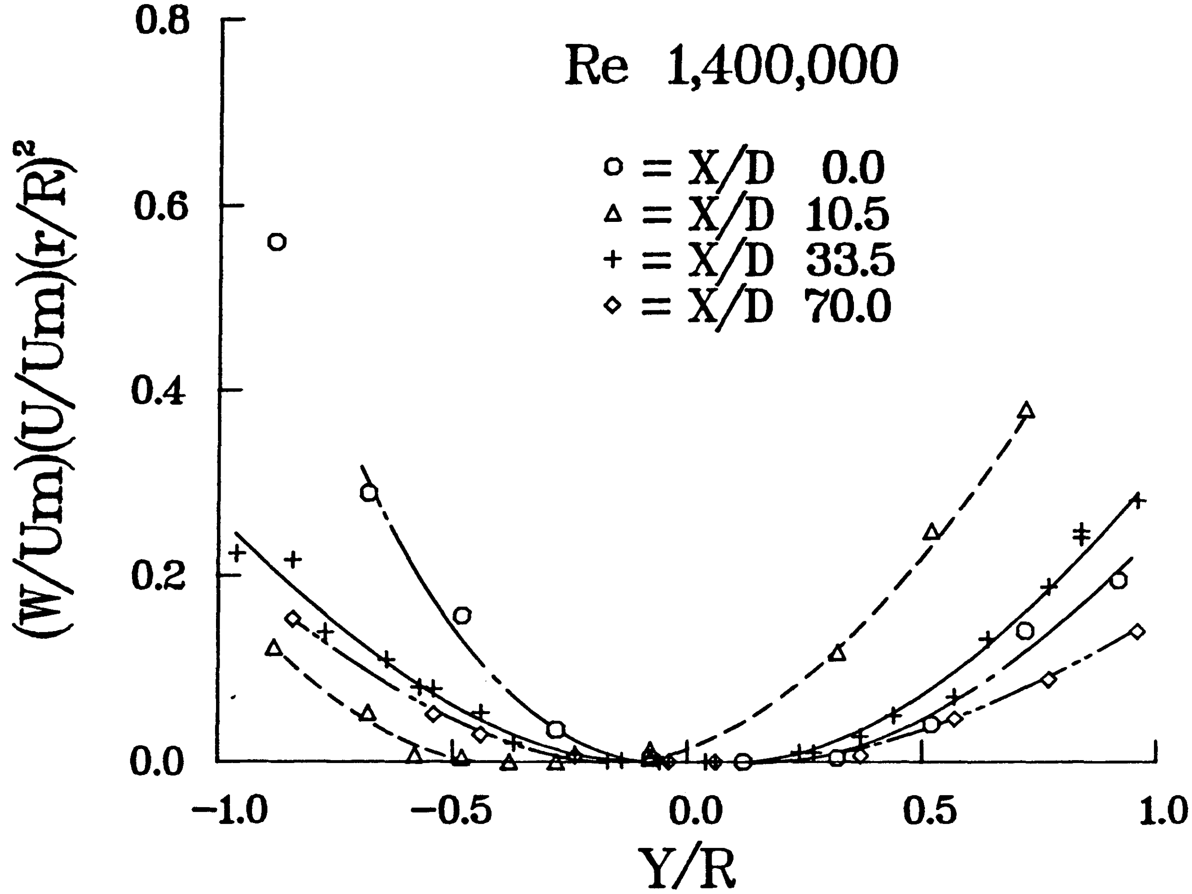

Figure 16. Angular momentum distribution at Re = 1,4000,000

more symmetric by 33.5D. At this location, profiles were made in the horizontal and vertical direction. The two profiles are quite similar.

Angular momentum flux profiles at all 3 pipe Reynolds numbers have similar characteristics as seen in figure 15 and 16. The swirl is markedly asymmetric at $x/D = 0.0$ and 10.5. The total angular momentum flux is the largest at the initial location and decays as the axial distance, x/D, increases. The angular momentum decays far more in the first 33.5 diameters and then the rate of decay decreases substantially between 33.5 and 70, which is characteristic of an exponential decay.

The tabulated values of the swirl angle, axial velocity, tangential velocity, and angular momentum flux at each radial position are given in Appendix I. Plots of the tangential velocity distributions are also presented in Appendix I.

VII NUMERICAL MODEL

Numerical models are useful in that the effect of different parameters can be evaluated more cost effectively on the computer than in the lab. If a model can be found that accurately describes the experimentally measured phenomena, the model would be of great use.

Fejer et al [1] derives a numerical model of the decay of the tangential component of velocity in swirling turbulent flow. The governing equation for the tangential velocity component is:

$$\mathrm{Re}\, U^{*} \frac{\partial W^{*}}{\partial z^{*}} = (1 + \varepsilon^{*}) \left[\frac{1}{r^{*}} \frac{\partial W^{*}}{\partial r^{*}} + \frac{\partial^{2} W^{*}}{\partial r^{*2}} - \frac{\partial W^{*}}{\partial r^{*}} + \frac{\partial^{2} W^{*}}{\partial z^{*2}} \right] \qquad (12)$$

where

$W^{*} = W/Um$

$U^{*} = U/Um$

$z^{*} = Z/R$

$r^{*} = r/R$

$\varepsilon^{*} = \varepsilon/\nu$

$\mathrm{Re} = \rho Um\ R/\nu$

Nissan and Bresan [8] showed that the radial component of velocity in swirling flow was orders of magnitude less than the tangential or axial components. The radial component was therefore neglected in the numerical model. The axial component was assumed constant in the axial direction. Figure 17 shows the axial velocity profile measured in swirling flow at three velocities. The velocities were normalized by the bulk average velocity, Um, determined from the mass flow reference system [14]. The profiles were measured with a conventional pitot tube that was designed to measure the resultant velocity. The conventional pitot tube is less subsecptable to scatter in the velocity measurement than the one used in the experimental portion for measuring swirl angles. The axial velocity profile used in the numerical model is shown as the continuous line in figure 17.

The fluid viscosity is assumed constant whereas the turbulent viscosity is a function of the flow. Kinney [15] determined a relationship for the eddy viscosity from Taylor's data in swirling flow to be

$$\varepsilon = K_4^2 \, r^2 \left| \frac{dW}{dr} - \frac{W}{r} \right| \tag{13}$$

where K_4 was found to be a "universal constant" equal to 0.028.

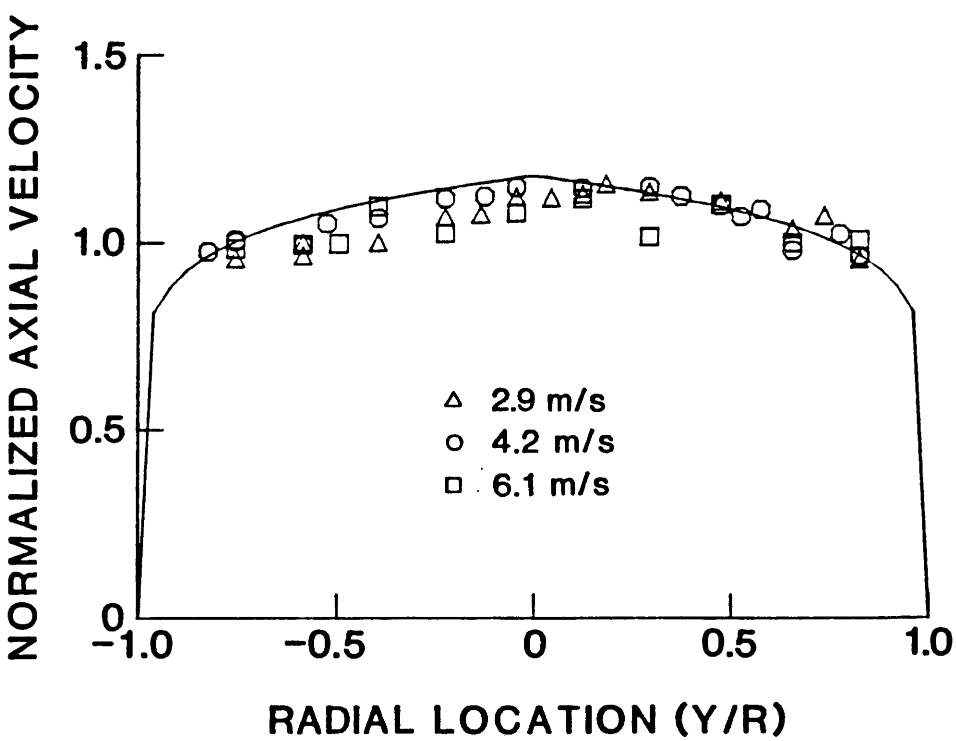

Figure 17. Axial velocity profile in swirling flow with power law profile used in numerical model

The decay of the tangential component of velocity in equation (12), was numerically analyzed with an explicit finite difference technique. The boundary conditions for equation (12) were :

$$W^* = 0 \quad @\ r^* = 0$$
$$W^* = 0 \quad @\ r^* = 1$$
$$W^* = f(r^*) \quad @\ z^* = 0$$

where $f(r^*)$ was a linear equation such that the maximum swirl angle was 29.5 degress on each side of the pipe or 59 degrees across the pipe. This is the average swirl measured in the experimental section at the initial position ($x/D = 0.0$).

A second boundary condition was necessary in the z-direction. Since there was not another known z boundary condition, the second derivative was not used until after the first time step. The grid pattern was $0.0125r^*$ in the z^* direction and $0.05r^*$ in the r^* direction. The coefficients on each finite difference element was positive, which satisfied the stability criterion for the model. The model was run at 3 different grid spacings in the z^* direction $-0.00125r^*$, $0.005r^*$, $0.0125r^*$ - without a significant difference in the results and therefore the convergence criterion was also satisfied.

The calculated swirl angles from the numerical model are shown in figure 18. The swirl continues to decay with increasing axial distance and appears exponential. After 300 diameters, the maximum swirl angle is greater than 9 degrees. The radial location of the maximum swirl angle translates towards the center of the pipe. The swirl takes on free and forced vortex characteristics which are different from what was experimentally measured. The calculated swirl does not decay as fast as the measured swirl.

The effect of the asymmetry of the swirl and of the pipe roughness were not considered in the computer model. The pipe used in the experimental portion of this study were "smooth" with a surface finish of approximately 70 μ inch.

Kreith and Sonju [7] analytical model of the decay of swirl neglected the second derivative of the tangential velocity with respect to distance, d^2W/dz^2. This was found to be insignificant in this computer model.

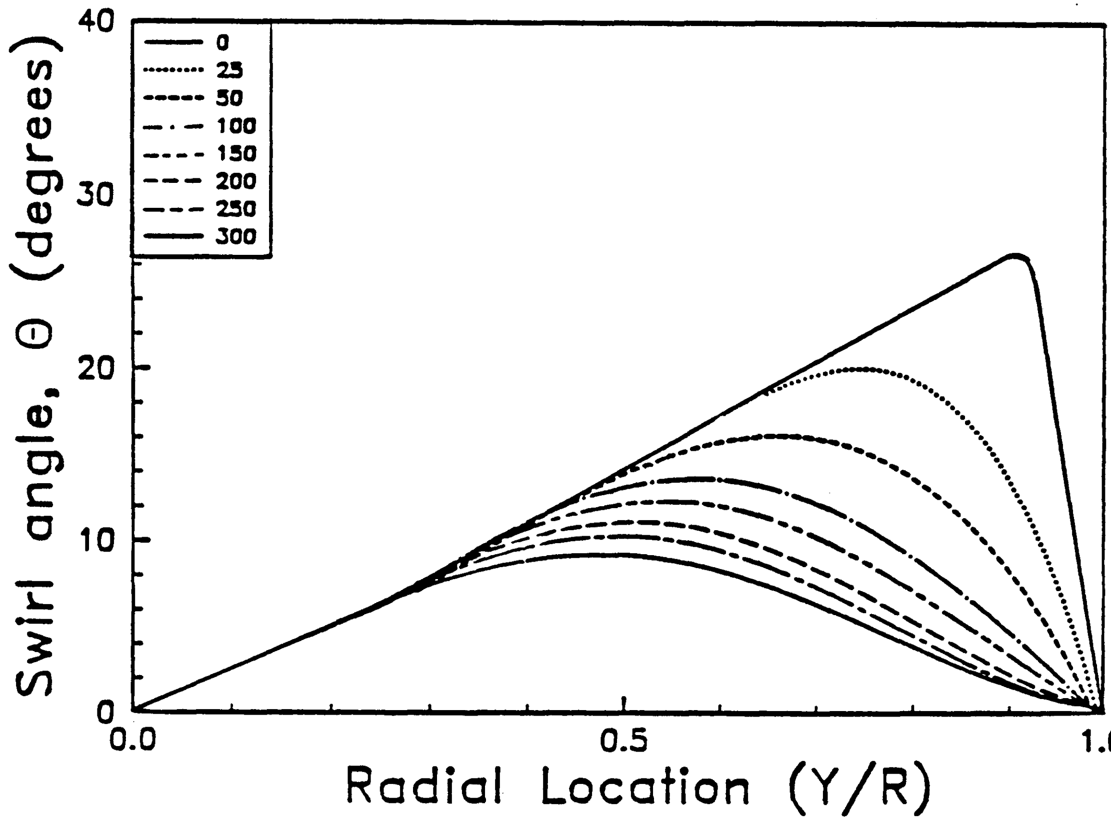

Figure 18. Swirl angle profiles at different axial locations, in pipe diameters, from numerical model

VIII DISCUSSION OF RESULTS

In this study, the best characteristic of the decay of swirling flow was the swirl angle. The average swirl angle on one side of the pipe, θ_{max} at each axial location is shown in figure 19. An exponential fit of the angular momentum using the experimental data is:

$$\frac{K}{K_o} = \frac{\tan(\theta_{max})}{\tan(\theta_{max})_{x/D=0}} = e^{-0.015\ x/D} \qquad (14)$$

Fejer, Lavan and Wolf [1] measured the decay of swirl in air in a 76mm (3 inch) pipe at 6 axial locations with pipe Reynolds numbers ranging from 80,000 to 360,000. Their decay correlation based on their data and numerical model shown previously is:

$$\frac{K}{K_o} = e^{-140\ Re^{-0.7}\ x/D} \qquad (15)$$

In this case, β is a function of Reynolds number:

$$\beta = 140\ Re^{-0.7}$$

Extrapolating to a pipe Reynolds number of 1,000,000, then β is 0.009 as compared to 0.015 for this study.

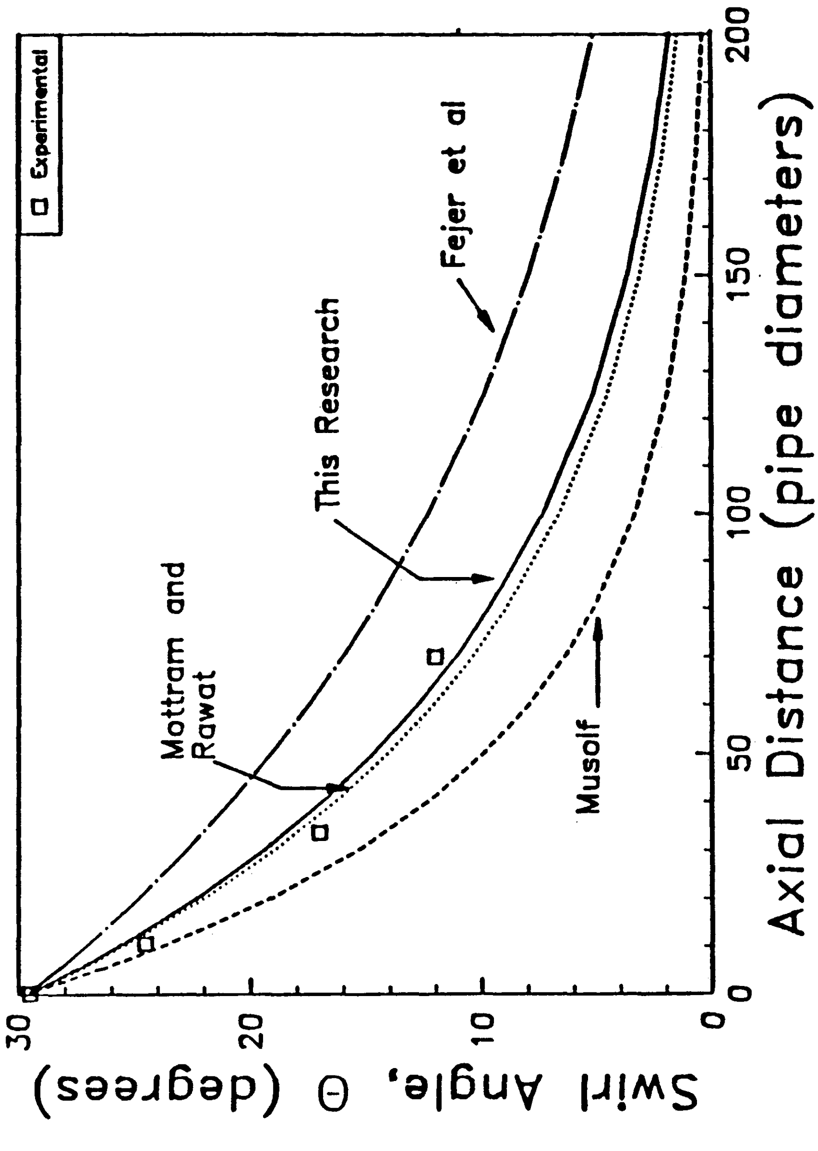

Figure 19. Swirl decay as a function of pipe length

Musolf [6] derived the following decay equation for water in the Reynolds number range of 20,000 to 120,000:

$$Sn = e^{-0.20\ Re^{-0.16}\ x/D} \tag{16}$$

β is 0.022 for a pipe Reynolds number of 1,000,000. Equations 14,15,16 are empirical exponential fits of the decay of angular momentum flux. Fejer's et. al. [1] data in air and Musolf's data in water show a strong Reynolds number dependence at low Reynolds numbers. As the Reynolds number increases the decay parameter, β, appears to decrease to a constant value. The decay rate is primarily a function of Reynolds number for Reynolds numbers below 1,000,000 and then approaches a constant. The friction factor also becomes independent of Reynolds number above a Reynolds number of a million [16]. Mottram and Rawat's [11] equation is a more complete equation, in that it accounts for both the Reynolds number and pipe roughness dependence in the friction factor. Figure 19 shows the predicted decay for Mottram and Rawat's [11] equation for a hydraulically smooth pipe with a friction factor of 0.0038. The predicted decay curves from Fejer [1], Musolf [6] and this research are also shown in figure 19.

IV CONCLUSIONS

Swirling flow can have a significant effect on flow meters. The common practice in the gas industry is to attenuate swirl and reduce flow disturbances with specified lengths of straight pipe. This study was intended to experimentally determine the rate of swirl decay at higher Reynolds numbers than have been previously reported in the literature. The decay was exponentially fit as a function of Reynolds number. Several other researchers [1,6] exponentially fit their lower Reynolds number data and their correlations bound the experimental results.

The conclusion of all the studies was that extremely long length of smooth pipe are required at Reynolds numbers greater than a million to attenuate swirl. In this study, over 50 pipe diameters are required to reduce 50% of the initial swirl. The Reynolds number is the primary effect controlling the decay rate in "smooth" pipes at low Reynolds numbers. As the Reynolds number increases the decay rate decreases to a constant value. At the relatively large Reynolds numbers reported in this study, there was not a statistically significant Reynolds number effect on the decay rate. Mottram and Rawat's [10] decay equation agrees well with the data and correlation shown here. Their form of the decay equation is more comprehensive than the other equations. By correlating the decay with the friction factor, the decay is not only a function of Reynolds number but also with pipe roughness. The friction factor also decreases to a constant value as the Reynolds number increases. In this study, the decay was only in smooth pipes, so no statement can be made as to the effect of roughness from the experimental data. Mottram and Rawat [11] have shown the required pipe lengths can be reduced significantly by roughening the pipes.

In order to remove swirl for improved flow measurement accuracy, flow straighteners should be installed upstream of the flowmeter or possibly rough sections of pipe can be used. More research is necessary to determined the required surface finish and to prevent the surface finish from adversely affecting the performance of the flowmeter.

REFERENCES

1. Fejer, A., Lavan, Z., and L. Wolf, Jr., Study of Swirling Fluid Flow, ARL 68-0713, Aerospace Research Laboratories, USAF, Wright-Patterson Air Force Base, Ohio (1968).

2. Kinghorn, F. C., Flow measurement in swirling or asymmetric flow- a review, Proceedings of Flow-Con. 77, Application of flow measuring techniques, Brighton, Sussex, 26-28 April 1977, pp. 45-74.

3. Bean, H. S., The effect on orifice meter indications of various pipe fittings near the orifice plate, Western Gas (1929).

4. McManus, S. E., B. R. Bateman, J. A. Brennan, I. Vazquez, and D. Mann, The Decay of Swirling Gas Flow in Long Pipes. American Gas Association 1985 Operating Section Proceedings, pp. 629-633, (1985).

5. American National Standards Institute, ANSI/API 2530, Orifice Metering of Natural Gas, American Gas Association, 1515 Wilson Boulevard, Arlington, Va. 22209 (1978).

6. Musolf, A. O., An Experimental Investigation of the Decay of Turbulent Swirl Flow in a Pipe, M.S. Thesis, University of Colorado, Dept. of Civil Engineering (1963).

7. Kreith, F. and O. K. Sonju, The Decay of a Turbulent Swirl in a Pipe, Journal of Fluid Mechanics, Vol. 22, Part 2, pp. 257-271 (1965).

8. Nissan, A. H., and V. P. Bresan, Swirling Flow in Cylinders, AIChE Journal, Vol. 7, No. 4, pp. 543-547 (1961).

9. Baker, D. W., Decay of Swirling, Turbulent Flow of Incompressible Fluids in Long Pipes, Ph. D. Thesis, University of Maryland (1967).

10. Baker, D. W., and C. L. Sayre, Decay of Swirling Flow of Incompressible Fluids in Long Pipes, Flow: Its Meas. and Control in Sci. and Ind., Sym. Proc., Pittsburgh, Pa., May 9-14, 1974.

11. Mottram, R. C. and M. S. Rawat, The Swirl Damping Properties of Pipe Roughness and the Implications for Orifice Meter Installation, Proceedings of the Flow Measurement in the Mid 80's International Conference, National Engineering Laboratory, Scotland, 29 pp., (June 1986).

12. Cheremisinoff, N. P., Fluid Flow, Pumps, Pipes and Channels, Ann Arbor Science, pp. 112-113 (1981).

13. Bryer, D. W. and R. C. Pankhurst, Pressure-probe methods for determining wind speed and flow direction, National Laboratory, Her Majesty's Stationary Office, London (1971).

14. Mann, D. B., and J. A. Brennan, On a new method of gas flow measurement using cryogenic techniques, National Bureau of Standards (U.S.), Special Publication 484, Vol. 2, pp 881-93, (1977).

15. Kinney, R. B., Universal velocity similarity in fully turbulent rotating flow, Paper No. 67-APM-23 - Applied Mechanics Conference of the ASME, Pasedena, California, June 26-28, 1967.

16. Moody, L. F., Friction factors for pipe flow, Transactions of the American Society of Mechanical Engineers, Vol. 66, No. 8, (November 1944).

APPENDIX I - Tabulated Values

Tables A1 to A14 are tabulated values of the experimental and calculated values of :

1) Fluid static pressure
2) Radial position, Y/R
3) Swirl angle, degrees
4) Normalized axial velocity, U/Um
5) Normalized tangential velocity, W/Um
6) Normalized angular momentum, $(U/Um)(W/Um)(r/R)^2$
7) Fluid temperature, K
8) Average bulk velocity, Um

at each axial location and pipe Reynolds number. The date of the experiment is also given as an identifier in column 1. The data has been sorted in increasing radial position even though the test plan was a random sequence.

Plots of the tangential velocity profiles at each axial location are presented in figures A1 to A5. The tangential velocity, W, is normalized by the average bulk velocity. The abscissa is a normalized distance from the center of the pipe.

Table A1. Tabulated values of vertical profile at $x/D = 0.0$ and $Re = 800,000$.

Fluid Temperature= 289.7 K   Um= 3.30 m/s

DATE	PRESSURE (MPa)	RADIAL POSITION (Y/R)	SWIRL ANGLE (deg.)	AXIAL VELOCITY	TANGENTIAL VELOCITY	ANGULAR MOMENTUM
850219	4.10	-.92	-20.0	1.06	0.39	0.49
850219	4.08	-.82	-21.0	0.91	0.35	0.31
850219	4.05	-.72	-20.0	1.23	0.45	0.44
850219	4.03	-.52	-19.0	0.74	0.26	0.09
850219	4.06	-.52	-19.0	0.93	0.32	0.14
850219	4.05	-.32	-17.0	0.80	0.24	0.05
850219	4.03	-.12	-12.0	0.64	0.14	0.01
850219	4.03	0.08	-4.0	0.77	0.05	0.00
850219	4.09	0.14	-2.0	0.23	0.01	0.00
850219	4.07	0.19	6.0	1.01	0.11	0.00
850219	4.04	0.29	8.0	1.53	0.22	0.00
850219	4.07	0.39	13.0	0.54	0.12	0.00
850219	4.04	0.49	18.0	1.18	0.38	0.05
850219	4.08	0.59	25.0	0.94	0.44	0.07
850219	4.04	0.69	30.0	0.52	0.30	0.04
850219	4.04	0.89	34.0	0.97	0.66	0.33
850219	4.09	0.99	33.0	0.82	0.53	0.30

Table A2. Tabulated values of vertical profile at x/D = 0.0 and Re = 1,000,000.

Fluid Temperature= 290.0 K   Um= 4.27 m/s

DATE	PRESSURE (MPa)	RADIAL POSITION (Y/R)	SWIRL ANGLE (deg.)	AXIAL VELOCITY	TANGENTIAL VELOCITY	ANGULAR MOMENTUM
840620	4.00	-.88	-26.0	0.85	0.41	0.39
840620	3.99	-.68	-26.0	1.11	0.54	0.43
840620	3.98	-.48	-25.0	0.88	0.41	0.15
840620	3.99	-.28	-21.0	0.73	0.28	0.04
840620	3.98	-.08	-15.0	0.72	0.19	0.01
840620	4.00	0.12	-2.0	0.48	0.02	0.00
840620	3.97	0.17	4.0	0.71	0.05	0.00
840620	3.98	0.32	15.0	0.21	0.06	0.00
840620	3.99	0.52	26.0	0.66	0.32	0.02
840620	3.98	0.72	32.0	0.82	0.51	0.13
840620	3.99	0.92	39.0	0.71	0.57	0.23

Table A3. Tabulated values of vertical profile at x/D = 0.0 and Re = 1,400,000.

Fluid Temperature= 290.0 K   Um= 5.79 m/s

DATE	PRESSURE (MPa)	RADIAL POSITION (Y/R)	SWIRL ANGLE (deg.)	AXIAL VELOCITY	TANGENTIAL VELOCITY	ANGULAR MOMENTUM
840622	3.84	-.88	-28.0	0.98	0.52	0.56
840622	3.83	-.68	-27.0	0.89	0.45	0.29
840622	3.81	-.48	-23.0	0.94	0.40	0.16
840622	3.83	-.28	-17.0	0.75	0.23	0.03
840622	3.82	-.08	-9.0	0.68	0.11	0.00
840622	3.83	0.12	3.0	0.66	0.03	0.00
840622	3.82	0.32	16.0	0.76	0.22	0.00
840622	3.82	0.52	24.0	0.86	0.38	0.04
840622	3.81	0.72	31.0	0.88	0.53	0.14
840622	3.82	0.92	33.0	0.73	0.47	0.19

Table A4. Tabulated values of vertical profile at x/D = 10.5 and Re = 800,000.

Fluid Temperature= 289.0 K Um= 2.88 m/s

DATE	PRESSURE (MPa)	RADIAL POSITION (Y/R)	SWIRL ANGLE (deg.)	AXIAL VELOCITY	TANGENTIAL VELOCITY	ANGULAR MOMENTUM
840626	4.00	-.88	-32.0	1.01	0.63	0.23
840626	4.00	-.68	-28.0	0.76	0.40	0.05
840626	4.00	-.48	-18.0			
840626	4.00	-.28	-2.0	0.19	0.01	0.00
840626	4.00	-.18	12.0	0.84	0.18	0.00
840626	4.00	-.08	5.0	0.89	0.08	0.00
840626	4.00	0.32	14.0	1.00	0.25	0.09
840626	4.00	0.52	17.0	0.74	0.22	0.11
840626	4.00	0.72	17.0	1.26	0.38	0.48

Table A5. Tabulated values of vertical profile at x/D = 10.5 and Re = 1,000,000.

Fluid Temperature= 290.0 K Um= 4.11 m/s

DATE	PRESSURE (MPa)	RADIAL POSITION (Y/R)	SWIRL ANGLE (deg.)	AXIAL VELOCITY	TANGENTIAL VELOCITY	ANGULAR MOMENTUM
840626	4.02	-.46	-19.0	0.38	0.13	0.00
840626	4.03	-.43	-16.0	0.44	0.13	0.00
840626	4.03	-.38	-10.0	0.65	0.11	0.00
840626	4.03	-.28	2.0			
840626	4.01	-.28	0.0	0.55	0.00	0.00
840626	4.03	-.08	16.0	1.01	0.29	0.01
840626	4.04	-.08	14.0	0.72	0.18	0.00
840626	4.04	0.32	18.0	0.90	0.29	0.09
840626	4.03	0.52	15.0	1.03	0.28	0.18
840626	4.04	0.72	15.0	1.06	0.28	0.30

Table A6. Tabulated values of vertical profile at x/D = 10.5 and Re = 1,400,000.

Fluid Temperature= 289.0 K   Um= 5.77 m/s

DATE	PRESSURE (MPa)	RADIAL POSITION (Y/R)	SWIRL ANGLE (deg.)	AXIAL VELOCITY	TANGENTIAL VELOCITY	ANGULAR MOMENTUM
840626	3.87	-.88	-41.0	0.63	0.55	0.12
840626	3.87	-.68	-36.0	0.68	0.49	0.05
840626	3.86	-.58	-29.0	0.38	0.21	0.01
840626	3.86	-.48	-19.0	0.60	0.21	0.00
840626	3.86	-.38	-9.0	0.26	0.04	0.00
840626	3.87	-.28	-1.0	0.43	0.01	0.00
840626	3.87	-.08	19.0	0.97	0.33	0.01
840626	3.86	-.08	12.0	0.67	0.14	0.00
840626	3.86	0.32	18.0	1.00	0.33	0.12
840626	3.87	0.52	18.0	1.09	0.35	0.25
840626	3.86	0.72	17.0	1.11	0.34	0.38

Table A7. Tabulated values of vertical profile at $x/D = 33.5$ and $Re = 800{,}000$.

Fluid Temperature= 290.0 K Um= 2.94 m/s

DATE	PRESSURE (MPa)	RADIAL POSITION (Y/R)	SWIRL ANGLE (deg.)	AXIAL VELOCITY	TANGENTIAL VELOCITY	ANGULAR MOMENTUM
840705	4.05	-.84	-15.0	0.58	0.16	0.06
840705	4.05	-.64	-16.0	0.98	0.28	0.11
840705	4.05	-.44	-13.0	0.91	0.21	0.04
840705	4.05	-.24	-8.0	0.82	0.12	0.00
840705	4.05	-.04	0.0	0.73	0.00	0.00
840705	4.05	0.17	3.0	1.17	0.06	0.00
840705	4.05	0.37	8.0	0.85	0.12	0.01
840705	4.05	0.57	10.0	0.92	0.16	0.05
840705	4.05	0.57	11.0	1.04	0.20	0.07
840705	4.06	0.77	12.0	1.12	0.24	0.16
840705	4.05	0.96	13.0	1.04	0.24	0.23

Table A8. Tabulated values of horizontal profile at x/D = 33.5 and Re = 800,000.

Fluid Temperature= 290.5 K   Um= 2.94 m/s

DATE	PRESSURE (MPa)	RADIAL POSITION (Y/R)	SWIRL ANGLE (deg.)	AXIAL VELOCITY	TANGENTIAL VELOCITY	ANGULAR MOMENTUM
840706	3.99	-.84	-17.0	0.98	0.30	0.21
840706	3.99	-.84	-17.0	0.86	0.26	0.16
840706	3.99	-.64	-16.0	0.97	0.28	0.11
840706	3.99	-.44	-15.0	0.69	0.18	0.02
840706	3.99	-.24	-10.0			
840706	3.99	-.04	-5.0	0.96	0.08	0.00
840706	3.99	0.06	-2.0			
840706	3.99	0.17	2.0	1.01	0.03	0.00
840706	3.99	0.27	4.0	0.64	0.04	0.00
840706	3.99	0.37	9.0	0.72	0.11	0.01
840706	3.99	0.57	12.0	0.93	0.20	0.06
840706	3.99	0.77	12.0	0.69	0.15	0.06
840706	3.99	0.96	14.0			

Table A9. Tabulated values of vertical profile at x/D = 33.5 and Re = 1,000,000.

Fluid Temperature= 290.0 K   Um= 4.17 m/s

DATE	PRESSURE (MPa)	RADIAL POSITION (Y/R)	SWIRL ANGLE (deg.)	AXIAL VELOCITY	TANGENTIAL VELOCITY	ANGULAR MOMENTUM
840705	4.01	-.84	-18.0	0.80	0.26	0.15
840705	4.03	-.64	-19.0	0.81	0.28	0.09
840705	4.03	-.44	-18.0	0.87	0.28	0.05
840705	4.03	-.24	-14.0	0.83	0.21	0.01
840705	4.03	-.04	-5.0	0.52	0.05	0.00
840705	4.02	0.17	6.0	0.66	0.07	0.00
840705	4.03	0.37	14.0	0.60	0.15	0.01
840705	4.03	0.57	16.0	0.97	0.28	0.09
840705	4.04	0.77	17.0	0.93	0.28	0.16
840705	4.03	0.96	17.0	0.99	0.30	0.28

Table A10. Tabulated values of horizontal profile at x/D = 33.5 and Re = 1,000,000.

Fluid Temperature= 290.5 K Um= 4.28 m/s

DATE	PRESSURE (MPa)	RADIAL POSITION (Y/R)	SWIRL ANGLE (deg.)	AXIAL VELOCITY	TANGENTIAL VELOCITY	ANGULAR MOMENTUM
840706	3.94	-.84	-16.0	0.98	0.28	0.19
840706	3.94	-.64	-16.0	1.04	0.30	0.13
840706	3.93	-.44	-16.0	1.09	0.31	0.07
840706	3.93	-.24	-14.0	0.92	0.23	0.01
840706	3.93	-.04	-9.0	0.84	0.13	0.00
840706	3.94	0.17	1.0	0.89	0.01	0.00
840706	3.93	0.27	8.0	0.82	0.11	0.01
840706	3.94	0.37	11.0	0.92	0.18	0.02
840706	3.93	0.47	12.0	0.82	0.17	0.03
840706	3.93	0.57	10.0	0.92	0.16	0.05
840706	3.94	0.77	14.0	0.98	0.24	0.14
840706	3.93	0.96	15.0	0.77	0.20	0.14

Table A11. Tabulated values of vertical profile at x/D = 33.5 and Re = 1,400,000.

Fluid Temperature= 290.0 K Um= 5.85 m/s

DATE	PRESSURE (MPa)	RADIAL POSITION (Y/R)	SWIRL ANGLE (deg.)	AXIAL VELOCITY	TANGENTIAL VELOCITY	ANGULAR MOMENTUM
840705	3.85	-.84	-18.0	0.97	0.32	0.22
840705	3.85	-.64	-19.0	0.88	0.30	0.11
840705	3.83	-.54	-20.0	0.86	0.31	0.08
840705	3.83	-.44	-19.0	0.89	0.31	0.05
840705	3.85	-.24	-14.0	0.75	0.19	0.01
840705	3.83	-.14	-11.0	0.71	0.14	0.00
840705	3.84	-.04	-4.0	0.75	0.05	0.00
840705	3.83	0.06	0.0	0.67	0.00	0.00
840705	3.85	0.17	4.0	0.81	0.06	0.00
840705	3.83	0.27	12.0	0.79	0.17	0.01
840705	3.84	0.37	14.0	0.89	0.22	0.03
840705	3.85	0.57	16.0	0.87	0.25	0.07
840705	3.84	0.77	17.0	1.02	0.31	0.19
840705	3.84	0.96	18.0	0.97	0.31	0.28

Table A12. Tabulated values of horizontal profile at x/D = 33.5 and Re = 1,400,000.

Fluid Temperature= 290.5 K   Um= 5.85 m/s

DATE	PRESSURE (MPa)	RADIAL POSITION (Y/R)	SWIRL ANGLE (deg.)	AXIAL VELOCITY	TANGENTIAL VELOCITY	ANGULAR MOMENTUM
840706	3.84	-.84	-20.0	0.98	0.36	0.25
840706	3.84	-.84	-20.0	0.97	0.35	0.24
840706	3.84	-.64	-21.0	0.92	0.35	0.13
840706	3.84	-.44	-20.0	0.84	0.31	0.05
840706	3.84	-.24	-16.0	0.80	0.23	0.01
840706	3.84	-.04	-6.0	0.65	0.07	0.00
840706	3.84	0.06	-1.0	0.78	0.01	0.00
840706	3.84	0.17	3.0	0.84	0.04	0.00
840706	3.84	0.37	11.0	0.87	0.17	0.02
840706	3.84	0.57	14.0	1.00	0.25	0.08
840706	3.84	0.77	15.0	0.94	0.25	0.14
840706	3.84	0.96	16.0	0.92	0.26	0.22

Table A13. Tabulated values of vertical profile at x/D = 70.0 and Re = 1,000,000.

Fluid Temperature= 287.0 K   Um= 4.19 m/s

DATE	PRESSURE (MPa)	RADIAL POSITION (Y/R)	SWIRL ANGLE (deg.)	AXIAL VELOCITY	TANGENTIAL VELOCITY	ANGULAR MOMENTUM
840817	4.01	-.84	-14.0	0.96	0.24	0.16
840817	4.01	-.64	-12.0	0.93	0.20	0.07
840817	4.01	-.44	-10.0	1.09	0.19	0.04
840817	4.01	-.24	-8.0	0.85	0.12	0.00
840817	4.01	-.04	-4.0	0.83	0.06	0.00
840817	4.01	0.06	-3.0	0.95	0.05	0.00
840817	4.01	0.12	-1.0	1.02	0.02	0.00
840817	4.01	0.17	-1.0	0.94	0.02	0.00
840817	4.01	0.22	-1.0	1.09	0.02	0.00
840817	4.01	0.37	3.0	1.13	0.06	0.01
840817	4.01	0.57	6.0	1.16	0.12	0.04
840817	4.01	0.77	8.0	1.04	0.15	0.09
840817	4.01	0.96	10.0	0.65	0.12	0.07

Table A14. Tabulated values of vertical profile at x/D = 70.0 and Re = 1,400,000.

Fluid Temperature= 290.0 K   Um= 5.81 m/s

DATE	PRESSURE (MPa)	RADIAL POSITION (Y/R)	SWIRL ANGLE (deg.)	AXIAL VELOCITY	TANGENTIAL VELOCITY	ANGULAR MOMENTUM
840817	3.91	-.84	-14.0	0.94	0.23	0.15
840817	3.91	-.54	-11.0	0.95	0.18	0.05
840817	3.91	-.44	-10.0	0.93	0.16	0.03
840817	3.91	-.24	-7.0	0.98	0.12	0.01
840817	3.91	-.04	-4.0	0.99	0.07	0.00
840817	3.91	0.17	0.0	0.95	0.00	0.00
840817	3.92	0.37	3.0	0.98	0.05	0.01
840817	3.92	0.57	8.0	1.01	0.14	0.05
840817	3.92	0.77	9.0	0.97	0.15	0.09
840817	3.91	0.96	11.0	0.89	0.17	0.14

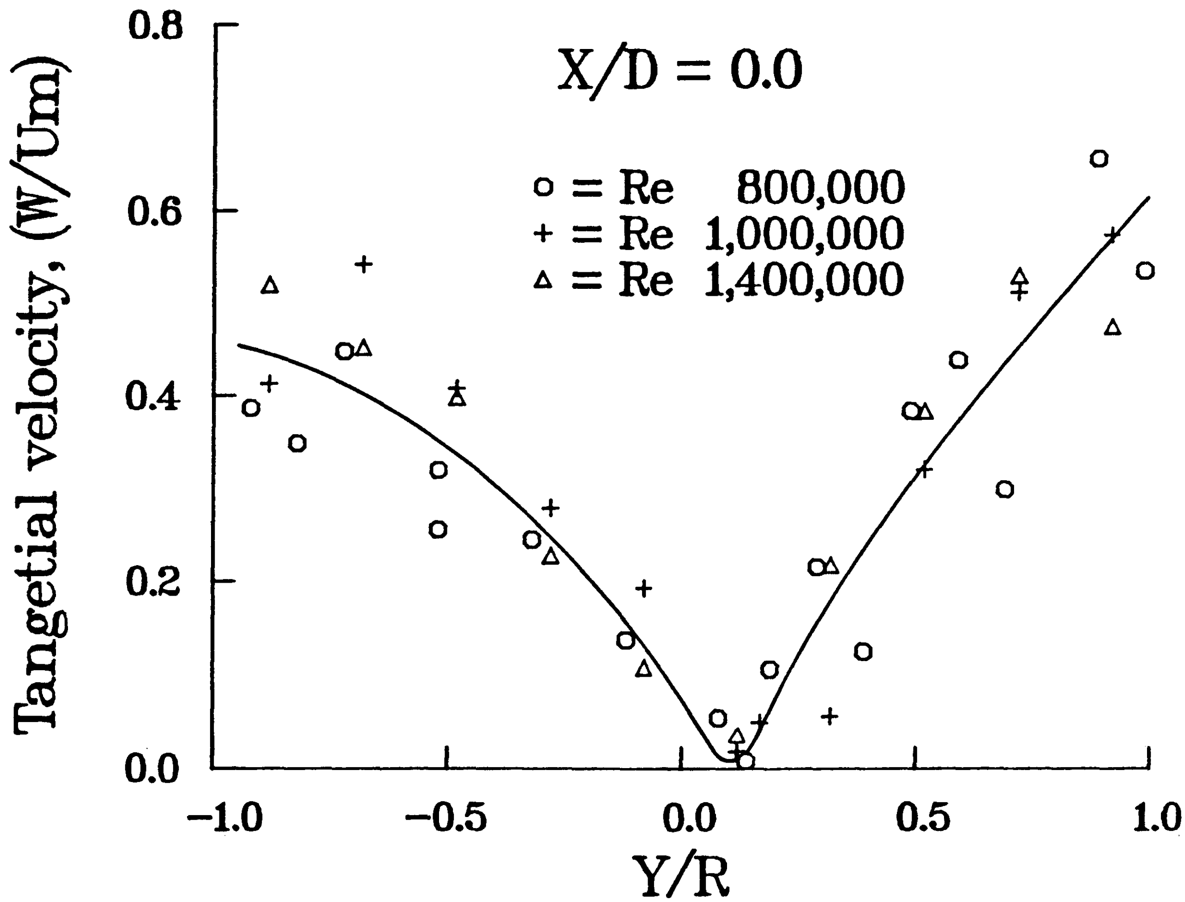

Figure A1. Tangential velocity profile of vertical traverse at x/D = 0.0

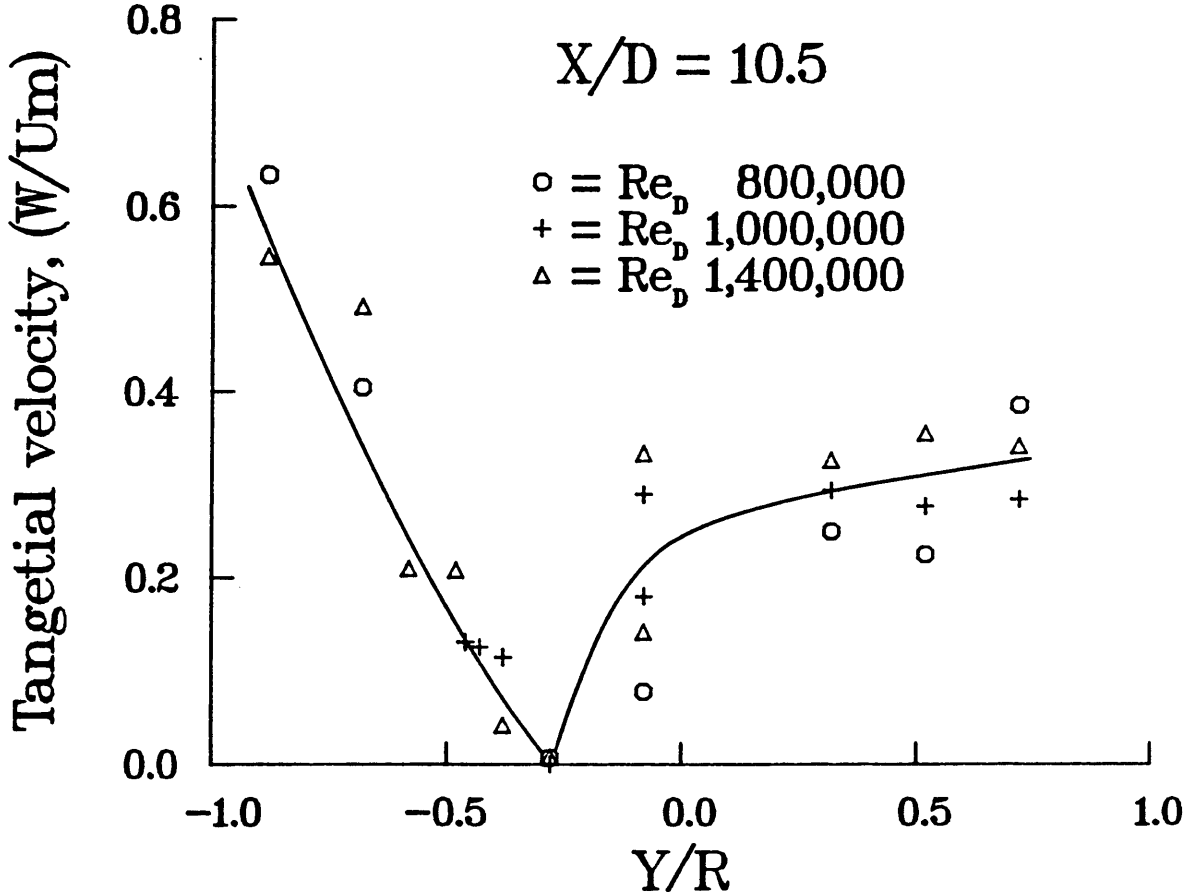

Figure A2. Tangential velocity profile of vertical traverse at x/D = 10.5

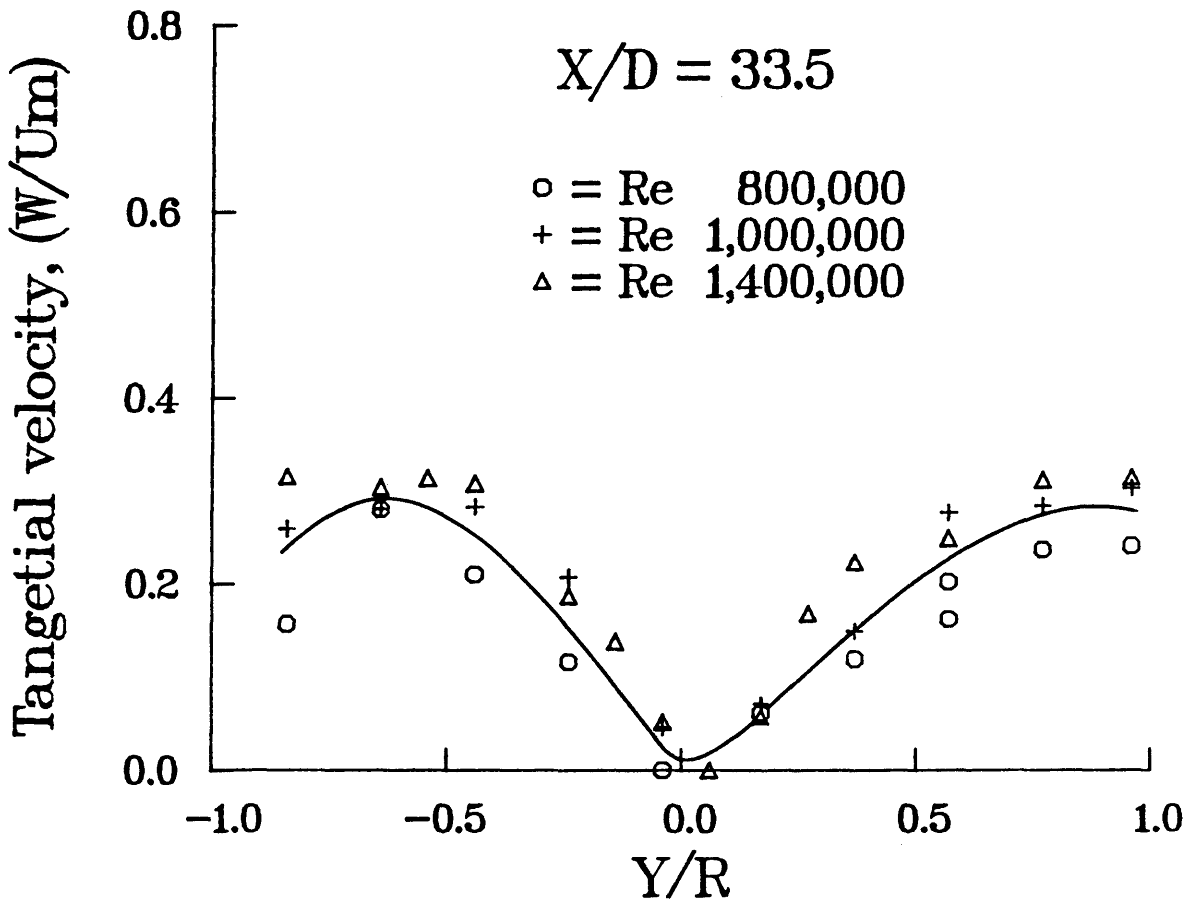

Figure A3. Tangential velocity profile of horizontal traverse at x/D = 33.5

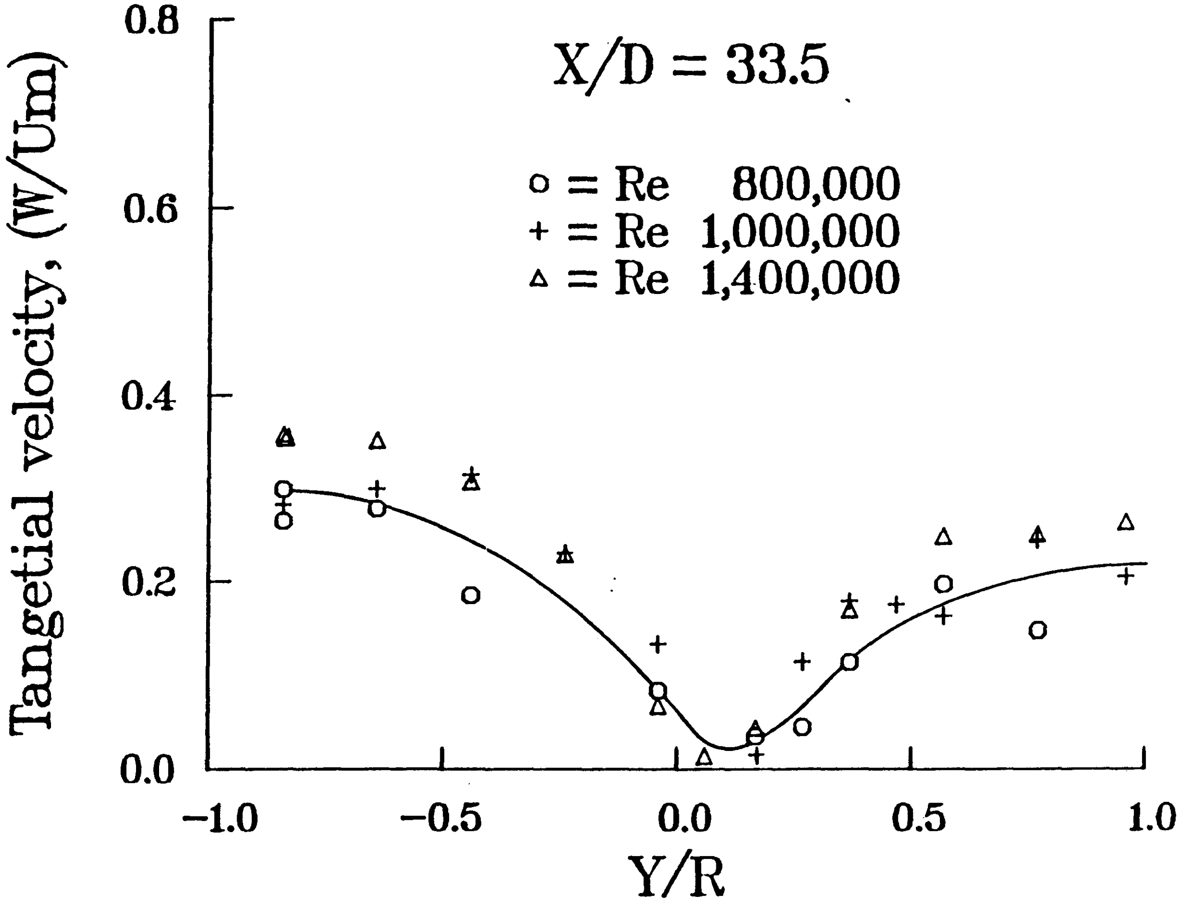

Figure A4. Tangential velocity profile of vertical traverse at x/D = 33.5

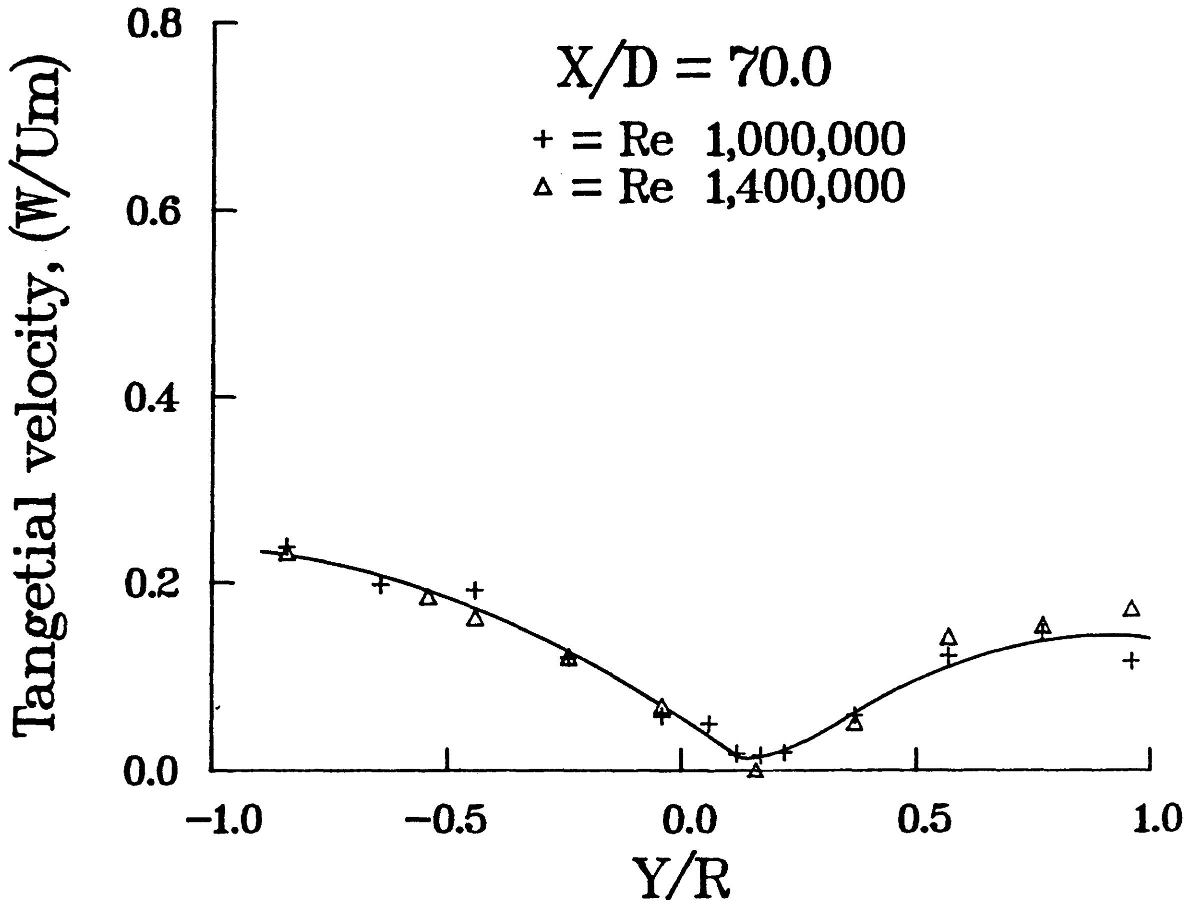

Figure A5. Tangential velocity profile of vertical traverse at x/D = 70.0